Polymer Degradation and Stability 230 (2024) 111050

Contents lists available at ScienceDirect

Polymer Degradation and Stability

journal homepage: www.journals.elsevier.com/polymer-degradation-and-stability

Synthesis and properties of poly (alkylene *trans*-1,4-cyclohexanedicarboxylate)s with different glycolic subunits

Giulia Guidotti [a], Clément Fosse [b], Michelina Soccio [a,c,d,*], Massimo Gazzano [e], Valentina Siracusa [f], Laurent Delbreilh [b], Antonella Esposito [b,*], Nadia Lotti [a,c,g]

[a] Department of Civil, Chemical, Environmental and Materials Engineering, University of Bologna, Via Terracini 28, 40131 Bologna, Italy
[b] Univ Rouen Normandie, INSA Rouen Normandie, CNRS, Groupe de Physique des Matériaux UMR 6634, F-76000 Rouen, France
[c] Interdepartmental Center for Industrial Research on Advanced Applications in Mechanical Engineering and Materials Technology, CIRI-MAM, Viale del Risorgimento 2, 40136 Bologna, Italy
[d] Interdepartmental Center for Industrial Research on Buildings and Construction, CIRI-EC, Via del Lazzaretto 15-5, 40131 Bologna, Italy
[e] Institute for Organic Synthesis and Photoreactivity, ISOF-CNR, Via Gobetti 101, 40129 Bologna, Italy
[f] Chemical Science Department, University of Catania, Viale A. Doria 6, 95125 Catania, Italy
[g] Interdepartmental Center for Agro-Food Research, CIRI-AGRO, Via Quinto Bucci 336, 47521 Cesena, Italy

ARTICLE INFO

Keywords:
Alicyclic
Odd-even effect
Mesophase
Polymorphism
Thermal analysis
Packaging
Biodegradability

ABSTRACT

This work explores one of the numerous playgrounds offered by polyesters. A series of poly (alkylene *trans*-1,4-cyclohexanedicarboxylate)s were synthesized combining *trans*-1,4-cyclohexane dicarboxylic acid with four diols containing an increasing number of methylene groups (n_{CH_2} = 3, 4, 5 and 6). The resulting polyesters are fully aliphatic. Their backbones contain cyclic aliphatic moieties and linear aliphatic segments in different relative contents depending on n_{CH_2}. The flexibility of these polyesters can be finely tuned (T_g decreases proportionally to the increase in n_{CH_2}), however the microstructure dramatically changes depending on whether n_{CH_2} is an odd or an even number (odd-even effect). On one hand, the odd-numbered samples are easier to melt-quench to a fully amorphous glassy state; on the other hand, the even-numbered samples are prone to crystallization and crystallize very fast. The developed microstructure is complex because of the probable coexistence of different crystalline structures, mesophases, and molecular arrangements depending on the *cis/trans* isomerism of the cyclohexane moiety. Preliminary tests provided mechanical and barrier properties that could make these polyesters suitable for packaging applications. Composting tests showed that increasing n_{CH_2} could eventually improve the biodegradation rate of these polyesters, although crystallinity remains the most influencing parameter.

1. Introduction

Polyesters offer an infinite variety of possibilities. They are easily obtained with petroleum-based reagents, but in many cases interesting alternatives can also be obtained from biomass. Polyesters can be aromatic, aliphatic, or contain moieties with both these characteristics. Melt polycondensation processes can be performed through the combination of a large panel of diacids and an even larger panel of diols. The most widespread, investigated, and industrially produced polyester is poly (ethylene terephthalate) (PET), whose repeating unit contains an aromatic 6-membered cyclic moiety associated with the shortest linear aliphatic glycolic subunit (2 methylene groups). The immediately successive homologuous polyesters of PET are poly (trimethylene terephthalate) (PTT, 3 methylene groups) and poly (butylene terephthalate) (PBT, 4 methylene groups). The general properties, preparation, and applications of PTT and PBT are reported in a recent book [1] and in a book's chapter [2], respectively. PPT is a semicrystalline aromatic polyester that was synthesized and patented in the 1940s and nowadays finds its main applications for the production of fibers. PBT was originally brought into the market as a replacement for phenolic resins in automotive applications in the mid-1970s; it has a much faster crystallization rate compared to PET, which differentiates it and opens the way to applications otherwise unsuitable for PET, such as injection-molding applications and fiber-containing semicrystalline composites. Indeed, the success of most engineering thermoplastic polymers is primarily attributed to high mechanical strength, toughness, fast crystallization rates allowing short processing cycle times, in some cases high heat distortion temperature and high continuous use temperature, dimensional and chemical stability [2]. The structure and the properties

* Corresponding authors.
E-mail addresses: m.soccio@unibo.it (M. Soccio), antonella.esposito@univ-rouen.fr (A. Esposito).

https://doi.org/10.1016/j.polymdegradstab.2024.111050
Received 7 September 2024; Received in revised form 18 October 2024; Accepted 20 October 2024
Available online 31 October 2024

of poly (alkylene terepthalate)s have been extensively investigated in the past [3], however synthetic strategies are still under development to make these polyesters perfectly suitable for applications [4] because the full potential of terephthalic polyesters with a number of methylene groups $n_{CH_2} > 4$ has not yet been disclosed.

In recent years, petroleum-based PET has been often challenged by biobased alternatives targeting the industry of packaging. The most credible candidate identified so far is biobased poly (ethylene furandicarboxylate) (PEF), whose barrier properties are even better than PET [5–7]. PEF contains an aromatic 5-membered heterocyclic moiety characterized by a strong dipolar moment [8], which explains its good barrier properties and provides an interesting pathway to control crystallinity, through the combination of controlled amounts of the position isomers 2,5- and 2,4-furandicarboxylic acid [9]. Poly (alkylene 2,5-furandicarboxylate)s with an increasing number of methylene groups are attracting attention [10–15], and some researchers are already investigating the possible end-of-life of furanic polyesters [16]. It is however interesting to explore solutions that (i) could potentially be biobased, (ii) have tunable microstructural, mechanical and barrier properties, and (iii) are eventually biodegradable in composting conditions, to comply with all sort of applications for which composting is the most likely-to-occur end-of-life (e.g. for food packaging). Unfortunately there are still many challenges to take up for biodegradable polymers to be used for practical packaging applications [17]. Aliphatic biodegradable polyesters with controlled chemical structures may help taking up at least a few of these challenges [18–20]. In some cases, the combination of aromatic and alicyclic moieties can provide synergistic effects on the functional properties [21].

This work investigates a series of poly (alkylene *trans*-1,4-cyclohexanedicarboxylate)s synthesized with *trans*-1,4-cyclohexane dicarboxylic acid and four diols containing an increasing number of methylene groups (n_{CH_2} = 3, 4, 5 and 6). The obtained polysters are fully aliphatic. They contain both cyclic moieties (with possible *cis/trans* isomerism) and linear sequences of increasing length. The investigations focused on their thermal stability, glass transition, aptitude to crystallize, mechanical properties, barrier properties to CO_2 and O_2, and compostability.

2. Materials and methods

2.1. Reagents

trans-1,4-cyclohexane dicarboxylic acid (CHDA) (96%, 4 mol% *cis*) was purchased from Zentek (Milan, Italy). 1,3-propanediol (PD) (98%), 1,4-butanediol (BD) (99%), 1,5-pentanediol (PeD) (96%), 1,6-hexanediol (HD) (99%) and titanium tetrabutoxide $Ti(OBu)_4$ (TBT) were purchased from Sigma-Aldrich. All the reagents and solvents used for the purification and precipitation processes (chloroform and methanol) were purchased from Sigma-Aldrich and used as received.

2.2. Synthesis

CHDA-based polyesters with different glycol subunits were synthesized via a two-step melt polycondensation process. CHDA and the selected glycol (1:1.2 molar ratio) were added in a thermoregulated and stirred glass reactor, together with $Ti(OBu)_4$ (200 ppm). During the first stage, the temperature was raised to 200 °C in nitrogen atmosphere and held constant until more than 90% of the theoretical amount of water was distilled off (about 2 h). Then, the pressure was reduced to about 0.1 mbar and the temperature was increased to 220 °C to remove the excess glycol. The polymerization was carried out until the torque reached a constant value. Finally, the synthetized polymers were discharged from the reactor and purified by dissolution in chloroform and precipitation in methanol. The as-obtained polymers appeared as white flocculates.

2.3. Molecular characterization

The chemical structure of the synthesized polyesters was evaluated by ^{1}H-NMR at room temperature with a Varian INOVA 400 MHz instrument (relaxation delay 1 s, acquisition time 1 s, 64 repetitions). The samples were dissolved in chloroform-d (5 mg ml^{-1}) with tetramethylsilane (0.03 vol%) as internal standard. The molecular weight and the dispersity of the synthesized polyesters were estimated by Gel Permeation Chromatography (GPC) using a 1100 Hewlett Packard system equipped with PL gel 5μ MiniMIX-C column at 30 °C eluted with chloroform (0.3 mL min^{-1}). The detection was made with the refractive index and the calibration curve was obtained with polystyrene standards (2000–100,000 g mol^{-1}). The poly (alkylene *trans*-1,4-cyclohexanedicarboxylate)s samples synthesized in this work are listed in Table 1 along with their molecular characteristics.

2.4. Modulated-Temperature Thermogravimetric Analysis (MT-TGA)

MT-TGA measurements were performed on a Discovery thermogravimetric analyzer (TA Instruments). Temperature and weight calibrations were made using nickel and weight standards. Experiments were achieved under a constant nitrogen flow of 20 mL min^{-1} to avoid oxidative degradation. Modulated-temperature heating ramps were carried out from room temperature to 600 °C with a modulation amplitude of ± 5 K, a heating rate of 2 K min^{-1} and an oscillation period of 60 s. The values of activation energy for the main degradation process were determined as a function of the conversion using a model-free method, as reported by Blaine et al. [22].

2.5. Differential Scanning Calorimetry (DSC)

Preliminary DSC measurements were performed by a calibrated DSC6 apparatus (Perkin Elmer). Samples weighing between 5 and 10 mg were encapsulated in aluminum pans, heated from −60 °C to a temperature 40 °C above their respective melting temperature with a heating rate of 20 K min^{-1} (1st scan), hold in isothermal conditions for 3 min, cooled down to −70 °C with a nominal cooling rate of 100 K min^{-1}, then heated again to the melt with a heating rate of 20 K min^{-1} (2nd scan).

2.6. Modulated-Temperature Differential Scanning Calorimetry (MT-DSC)

MT-DSC experiments were run on a DSC Q100 (TA Instruments) using the Tzero technology. The equipment was calibrated in temperature, energy and heat capacity using indium and sapphire standards. All the measurements were performed under a nitrogen flow of 50 mL min^{-1} to avoid oxidative degradation. The sample masses ranged between 5 and 10 mg. Prior to measurement, the samples were melted on a hot plate at a temperature above their respective melting temperatures, and then quenched in liquid nitrogen. After melt quenching, the samples were characterized with a heat-only protocol starting from −70 °C to a temperature above melting, with a heating rate of 2 K min^{-1}, an amplitude of modulation of ±0.32 K, and an oscillation period of 60 s, as recommended in the literature [23].

2.7. Fast Scanning Calorimetry (FSC)

FSC measurements were performed on a Flash DSC 1 (Mettler-Toledo) equipped with a HUBER TC 100 intracooler. Prior to use, each MultiSTAR UFS1 MEMS empty chip was conditioned and corrected as recommended by the manufacturer. A constant nitrogen flow of 200 mL min^{-1} was used during conditioning, correction and measurement, to prevent oxidative degradation. Samples with masses ranging between 30 and 130 ng were used for measurement. In the case of PPCE and

Table 1
List of poly (alkylene *trans*-1,4-cyclohexanedicarboxylate)s (PCHs) synthesized with CHDA and four different diols (PD, BD, PeD ans HD), along with their repeating unit, the molar mass of their repeating unit (M_0), the number-average molecular weight ($\overline{M}_n$), the weight-average molecular weight ($\overline{M}_w$), the dispersity ($Đ$), the degree of polymerization (DP_n) and the percentage of *cis*-isomers.

SAMPLE	UNIT	M_0 (g mol^{-1})	$\overline{M}_n$ (g mol^{-1})	$\overline{M}_w$ (g mol^{-1})	$Đ$	DP_n	*cis* (mol%)
PPCE	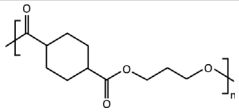	212	46,200	83,160	1.8	218	10
PBCE	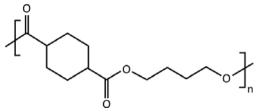	226	57,100	131,330	2.3	253	10
PPeCE	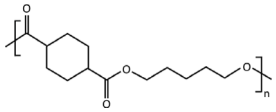	240	34,000	71,400	2.1	142	8
PHCE	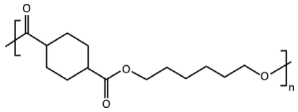	254	50,700	116,610	2.3	200	6

CHDA = *trans*-1,4-cyclohexane dicarboxylic acid (CHDA)
PD = 1,3-propanediol
BD = 1,4-butanediol
PeD = 1,5-pentanediol
HD = 1,6-hexanediol
PPCE = poly (propylene *trans*-1,4–cyclohexanedicarboxylate)
PBCE = poly (butylene *trans*-1,4–cyclohexanedicarboxylate)
PPeCE = poly (pentamethylene *trans*-1,4–cyclohexanedicarboxylate)
PHCE = poly (hexamethylene *trans*-1,4–cyclohexanedicarboxylate).

PPeCE, for which it was possible to obtain amorphous MT-DSC samples, the mass of FSC samples was estimated according to Eq. (1).

$$m = \frac{\Delta C_{p_{am}}^{FSC}[\mathrm{J\,K^{-1}}]}{\Delta c_{p_{am}}^{MT-DSC}[\mathrm{J\,g^{-1}\,K^{-1}}]} \quad (1)$$

Where $\Delta C_{p_{am}}^{FSC}[\mathrm{J\,K^{-1}}]$ is the heat capacity step of a fully amorphous nanoscale sample measured at the glass transition temperature by FSC ($\beta^+ = 1000$ K s^{-1}) and $\Delta c_{p_{am}}^{MT-DSC}[\mathrm{J\,g^{-1}\,K^{-1}}]$ is the specific heat capacity step of a fully amorphous bulk sample measured at the glass transition temperature by MT-DSC ($\beta^+ = 0.033$ K s^{-1}). In the case of PBCE and PHCE, as it was not possible to obtain amorphous MT-DSC samples, the mass of FSC samples was estimated following the procedure reported by Cebe et al. [24] (Eq. (2)).

$$m = \frac{C_p^{FSC}(T_1)[\mathrm{J\,K^{-1}}]}{c_p^{MT-DSC}(T_1)[\mathrm{J\,g^{-1}\,K^{-1}}]} \quad (2)$$

Where $C_p^{FSC}(T_1)[\mathrm{J\,K^{-1}}]$ is the heat capacity obtained from FSC measurements at the temperature T_1 and $c_p^{MT-DSC}(T_1)[\mathrm{J\,g^{-1}\,K^{-1}}]$ is the specific heat capacity measured by MT-DSC at the same temperature. The temperature T_1 was selected in the liquid state and the calculation was repeated for several temperature values over a wide temperature range to get an average of the sample mass. FSC samples were submitted to different cooling rates from temperatures above their respective melting with the purpose of approaching the critical cooling rate necessary to obtain fully amorphous samples. The reference values of melting enthalpies ΔH_m^0 (melting enthalpy of an hypothetical 100% crystalline sample) were then estimated using the protocol reported by Fosse et al. [25].

2.8. X-ray measurements

Wide-angle X-ray measurements were performed using a PANalytical X'Pert PRO diffractometer equipped with an X'Celerator detector and Cu anode as X-ray source ($\lambda_1 = 0.15406$ nm, $\lambda_2 = 0.15443$ nm). The measurements were performed at room temperature. The crystallinity X_C was determined as the ratio of the area below the crystalline diffraction peaks to the total area under the trace. The experimental data were treated with the High ScorePlus software package provided by Panalytical, and their analysis was performed using OriginLab fitting routines. The crystalline peaks were fitted with a Gaussian function each; the amorphous halo was fitted with two partially overlapping Gaussian functions, similarly to what previously done by Murthy et al. [26] for poly(ethylene terepththalate), and Stoclet et al. [27] for polylactide. The average size of the crystalline domains l_C was estimated perpendicularly to different crystalline plans using Scherrer's equation [28] (Eq. (3)).

$$l_C = \frac{K\lambda}{\beta cos\theta} \quad (3)$$

Where K is a dimensionless shape factor (0.89), λ is the X-rays wavelength (0.154 nm), β is the Full Width at Half Maximum (FWHM) of the selected crystalline peak, and θ is the Bragg's angle. The corresponding crystalline interplanar distance d was calculated with the Bragg's law [29] (Eq. (4)).

$$d = \frac{n\lambda}{2sin\theta} \quad (4)$$

Where n is an integer. This equation was also used to estimate the most representative average intrachain spacings in the amorphous phase, with 2θ corresponding to the angular positions of the amorphous halos.

2.9. Preparation and characterization of the films

Thin films of the synthesized polymers were obtained by compression molding. The polymer samples were placed between two Teflon plates and heated at $T = T_m + 40$°C, then 2 tons m^{-2} were applied for 2 min using a laboratory press (Carver C12). The films were ballistically cooled down to room temperature and stored at 25 °C for 2 weeks to stabilize the microstructure.

The thickness of each polymer film was measured using a Sample Thickness Tester DM-G with a digital dial indicator (MarCartor 1086,

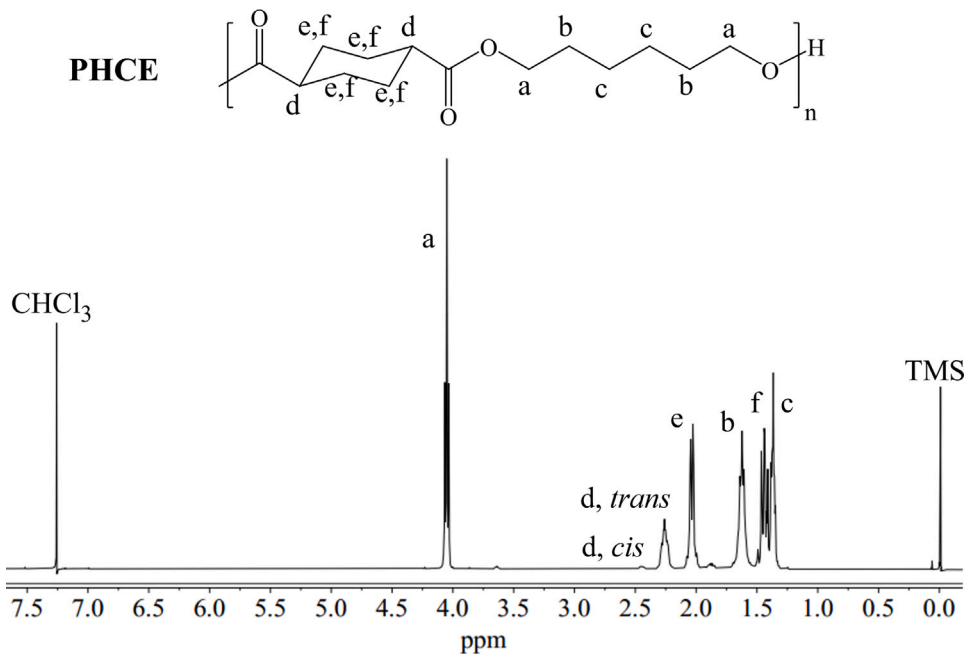

Fig. 1. ^{1}H-NMR spectrum of PHCE with the corresponding peak assignment.

Mahr GmbH, Esslingen, Germany) and the associated DM-G software. The reading was made twice per second with a resolution of 0.001 mm. The minimum, maximum, and average values for each reading were recorded in triplicates, in 10 different positions of each film, at room temperature, and reported as a mean value expressed in micrometers ± standard deviation.

2.10. Tensile tests

Tensile tests were performed on the polymer films using an Instron 5966 machine equipped with a rubber grip and a transducer-coupled 1 kN load cell. The polymer films were cut in rectangular strips (5 × 50 mm^2) and stretched with a 10 mm min^{-1} crosshead speed. The elastic modulus was calculated from the slope of the initial linear portion of the stress–strain curves. 7 replicate specimens were tested, providing the results as the average value ± standard deviation.

2.11. Gas permeability tests

Permeability tests were performed by a manometric method employing a Permeance Testing Device type GDP-C (Brugger Feinmechanik GmbH, Munich, Germany), according to ASTM 1434-82 (Standard Test Method for Determining Gas Permeability Characteristics of Plastic Film and Sheeting), DIN 53 536 in compliance with ISO/DIS 15 105-1, and according to Gas Permeability Testing Manual (Registergericht München HRB 77020, Brugger Feinmechanik GmbH). The measurements were carried out at 23 °C on samples having a surface of 78.5 cm^2 with a gas stream of 100 cm^3 min^{-1} in dry conditions (0% RH). The chamber and sample temperatures were controlled by an external thermostat KAAKE-Circulator DC10-K15 (ThermoFisher Scientific, Waltham, MA, USA). High-purity (100%) O_2 and CO_2 gases were used. The analyses were done using Method A as described in Brugger manual, with evacuation of both top and bottom chambers. The films were placed between the two chambers, as previously described by Siracusa and Ingrao [30], and the amount of gas flowing through the films was determined from the pressure variation due to the gas accumulation in the closed downstream chamber. The Gas Transmission Rate (GTR, cm^3 cm/m^2 d atm) was determined considering the pressure increase in relation to the time and volume of the device. The time lag (t_L, s), diffusion coefficient (D, cm^2 s^{-1}), and solubility (S, cm^3 cm^{-3} bar) were also measured. The mathematical relations used for calculations have been previously reported in the literature [31–34]. The measurements were carried out in triplicates and the results are provided as the average value ± standard deviation.

2.12. Composting tests

Composting tests have been performed using square films (30 × 30 mm^2) placed at 58 °C in a 100-mL bottle together with 20 g of compost kindly supplied by Gardea (Villa Franca, Italy) and 10 mL of deionized water. Water has been regularly added over time to keep the compost moist. After different times of incubation, the samples were withdrawn from the compost, cleaned, and dried under vacuum until reaching a constant weight [35]. The percentage weight loss was calculated as follows:

$$\%weightloss = \frac{(m_i - m_f)}{m_i} \times 100 \quad (5)$$

Where m_i and m_f are the initial and final sample weight, respectively. The tests were carried out in triplicates and the weight losses are provided as the average value ± standard deviation.

2.13. Scanning Electron Microscopy (SEM)

SEM observations were made by a Phenom microscope (Amsterdam, The Netherlands) to investigate the topography of the sample surfaces. Prior to analysis, the samples were cut to the right size and fixed with carbon tape on aluminum stubs, then sputtered with a gold thin film.

3. Results and discussion

3.1. Molecular characterizations

The chemical structure and the *cis*-isomer content of the synthesized polyesters were determined by ^{1}H-NMR spectroscopy. The spectra confirmed the expected structures and excluded the occurrence of side reactions during the polymerization process. As an example, Fig. 1 shows the ^{1}H-NMR spectrum of PHCE with the corresponding peak assignment. The signals at 4.05, 1.62 and 1.43 ppm are ascribed to

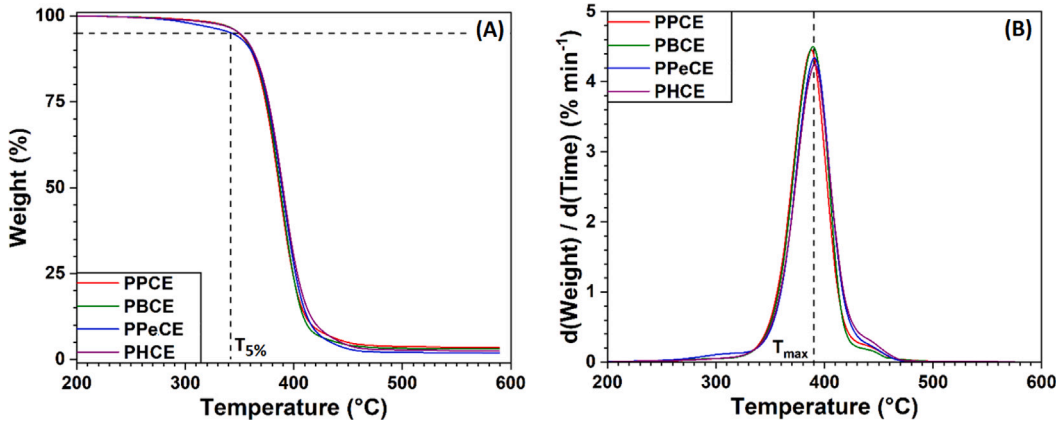

Fig. 2. (A) Degradation curves recorded by MT-TGA from room temperature to 600 °C with a modulation amplitude of ± 5 K, an overall heating rate of 2 K min^{-1} and an oscillation period of 60 s under a constant flow of nitrogen gas. $T_{5\%}$ is the temperature at which a weight loss of 5% is observed. (B) Derivative MT-TGA curves showing the temperature corresponding to the maximum rate of weight loss (T_{max}).

the *a*, *b* and *c* protons of the glycol subunit, respectively. Regarding the cyclohexane ring, the axial and equatorial protons (*e* and *f*) resonate at 2.05 and 1.40 ppm, respectively. Two kinds of *d* protons are detected, the first at 2.28 ppm for *trans*-isomers, and the second at 2.44 ppm for *cis*-isomers. Analogously, the ^{1}H-NMR spectra of the other polyesters synthesized in this work show similar characteristic peaks. PPCE: δ 4.10 ppm (4H, m); δ 2.45 ppm (2H, m); δ 2.30 ppm (2H, m); δ 2.05 ppm (4H, m); δ 1.90 ppm (2H, m); δ 1.47 ppm (4H, m). PBCE: δ 4.10 ppm (4H, m); δ 2.40 ppm (2H, m); δ 2.28 ppm (2H, m); δ 2.05 ppm (4H, m); δ 1.60 ppm (4H, m); δ 1.47 ppm (4H, m). PPeCE: δ 4.10 ppm (4H, m); δ 2.40 ppm (2H, m); δ 2.28 ppm (2H, m); δ 2.05 ppm (4H, m); δ 1.60 ppm (4H, m); δ 1.47 ppm (4H, m); δ 1.40 ppm (2H, m).

3.1.1. *cis-trans isomerism*

From the relative integral of the *d,cis* and *d,trans* signals, the *cis*-isomer content was calculated for all the samples and reported in Table 1. The *cis/trans* ratio strongly influences the properties of the obtained polymer, such as its characteristic thermal transitions, its ability to crystallize, and consequently its mechanical and barrier properties [36,37]. The *cis*-isomers have their two functions on the same side of the cyclohexane ring, whereas the *trans*-isomers have them on opposite sides; the *trans*-isomers are more regular and prefer being in a chair conformation, whereas the *cis*-isomers tend to arrange in a boat conformation, with an obvious disruptive role [37]. Therefore, a control over the relative amount of the two isomers is crucial. A slight increase in the *cis/trans* ratio with respect to the feed (4 mol % *cis*) could be due to the high temperatures used for the synthesis, which can prone a certain degree of isomerization, but which are also necessary to obtain high-molecular-weight polymers. Table 1 reports the number-average molecular weight ($\overline{M}_n$), the weight-average molecular weight ($\overline{M}_w$), the degree of polymerization (DP$_n$) and the dispersity ($Đ$) of all the synthesized polyesters. The high values of $\overline{M}_n$, associated with a value of $Đ$ close to 2 in all cases, confirm that the polymerization process was well controlled. It is worth noting that obtaining high-molecular-weight polymers is mandatory for processing self-sustaining films suitable to investigate the tensile mechanical behavior and the gas barrier properties.

3.2. *Thermal characterizations*

3.2.1. *Thermal stability*

MT-TGA allows to estimate the mass loss of a sample as a function of the temperature at which it is exposed, while providing the activation energy for thermal decomposition as a function of the degree of conversion α with a single measurement in conditions of temperature modulation [22,38,39]. Fig. 2 shows the weight change as a function of temperature measured by MT-TGA under a constant flow of nitrogen gas. All the samples exhibit one main degradation step. Their thermal stability was evaluated by considering the temperature at which a weight loss of 5% is observed ($T_{5\%}$), as well as the temperature at which the maximum rate of weight loss is measured (T_{max}). The MT-TGA data shown in Fig. 2 were also used to calculate the activation energy of the main degradation process using a model-free method, as reported in the literature [14,22].

The values of $T_{5\%}$ and T_{max} reported in Table 2 show that, in the selected conditions, the thermal stability of CHDA-based polyesters synthesized with different diols is not significantly affected by the number of methylene groups (n_{CH_2} = 3, 4, 5 and 6) introduced in the polymer backbone. Previous works had already investigated the thermal stability of thermoplastic polyesters as a function of n_{CH_2}. The number of methylene groups in the backbone of a polyester can be controlled by selecting either diols and/or diacids with different lengths to be combined through polycondensation. Depending on the selected reagents, the obtained polyester can either contain an aromatic moiety (as in the case of furanoate polyesters [10–14]), or be linear aliphatic (if they contain no cyclic moieties at all, as in the case of poly(alkylene succinate)s [40]), or contain a cyclic moiety that is aliphatic too, which is the case of the poly (alkylene cyclohexanoate)s investigated in this work. For comparison purposes, Table 2 reports some values issued from the literature for at least one example per type of polyester (alicyclic, aromatic, linear aliphatic) as a function of n_{CH_2}. Comparisons should be made only within each series of polyesters, because the values reported in the literature are often obtained with different heating rates (20 or 10 K min^{-1}) compared to this work, where a much slower heating rate was used as required by temperature modulation (2 K min^{-1}). It is interesting to see that the thermal stability of aliphatic polyesters, whether they contain or not a cyclic moiety in their repeating unit, seems to be generally very good and not significantly affected by the number of methylene groups n_{CH_2}, whereas the thermal stability of aromatic polysters strongly depends on the ratio of the aromatic/aliphatic segments in the repeating unit (the longer the aliphatic segment, the poorer the thermal stability), at least for $n_{CH_2} \leq 4$. The presence of aromatic moieties in a polymer backbone has generally been considered as an advantage for thermal stability with respect to aliphatic moieties. Interestingly, the value of activation energy obtained for poly (alkylene cyclohexanoate)s is comparable to the values reported in the literature for aromatic polyesters, such as poly (ethylene terephthalate) (PET) (227 kJ mol^{-1} [41]), poly (ethylene 2,5-furandicarboxylate) (2,5-PEF) (190 ± 25 kJ mol^{-1} [14], 180 ± 13 kJ mol^{-1} [10]) and poly (ethylene 2,4-furandicarboxylate) (2,4-PEF) (198 ± 10 kJ mol^{-1} [14]), and significantly larger than the values reported in the literature for one of the most widespread linear aliphatic polyesters, poly (lactic acid) (PLA) (110 kJ mol^{-1} [41] and 120 kJ mol^{-1} [42]).

Table 2
Parameters associated with thermal degradation under nitrogen gas. $T_{5\%}$ is the temperature at which a weight loss of 5% is observed, T_{max} is the temperature at which the rate of weight loss is maximum, and E_a is the activation energy of thermal decomposition. Analogous values about a few additional series of polyesters with a variable number of methylene groups n_{CH_2} in their backbone are also reported from the literature for comparison purposes.

SAMPLE	n_{CH_2}	$T_{5\%}$ (°C)	T_{max} (°C)	E_a (α = 0.5) (kJ mol^{-1})	REFERENCE Heating rate
PPCE	3	349 ± 3	388 ± 1	187 ± 4 (model-free)[a]	This work
PBCE	4	350 ± 3	389 ± 1	183 ± 6 (model-free)[a]	2 K min^{-1}
PPeCE	5	342 ± 3	390 ± 1	183 ± 10 (model-free)[a]	
PHCE	6	350 ± 3	391 ± 1	182 ± 7 (model-free)[a]	
2,5-PEF	2	339	411	190 ± 25 (model-free)[b]	Thiyagarajan et al. [14]
2,5-PPF	3	330	405	167 ± 35 (model-free)[b]	10 K min^{-1}
2,5-PBF	4	304	367	151 ± 10 (model-free)[b]	
2,4-PEF	2	345	429	198 ± 10 (model-free)[b]	Thiyagarajan et al. [14]
2,4-PPF	3	342	415	158 ± 26 (model-free)[b]	10 K min^{-1}
2,4-PBF	4	328	402	182 ± 9 (model-free)[b]	
PEF	2	375	416	180 ± 13 (Friedman) 133 ± 8 (Kissinger–Akahira–Sunose)	Tsanaktsis et al. [10] 20 K min^{-1}
PPF	3	366	394	115 ± 13 (Friedman) 129 ± 7 (Kissinger–Akahira–Sunose)	
PBF	4	340	362	175 ± 12 (Friedman) 97 ± 14 (Kissinger–Akahira–Sunose)	
PPeF	5	361	394	n.a.	Terzopoulou et al. [11]
PHF	6	356 [11], 360 [13]	389 [11], 391 [13]	131 ± 11 (Friedman) 114 ± 15 (Starink)	Papageorgiou et al. [13] 20 K min^{-1}
PNF	9	375	397	n.a.	
POF	8	368	n.a.	142 ± 15 (Kissinger–Akahira–Sunose)	Terzopoulou et al. [12]
PDeF	10	373	n.a.	140 ± 11 (Kissinger–Akahira–Sunose)	20 K min^{-1}
PDoF	12	363	n.a.	157 ± 7 (Kissinger–Akahira–Sunose)	
PESu	2	356	428	n.a.	Bikiaris et al. [40]
PBSu	4	350	422	n.a.	20 K min^{-1}
PHSu	6	319	425	n.a.	
POSu	8	328	426	n.a.	
PDeSu	10	333	429	n.a.	

PPCE, PBCE, PPeCE, PHCE = poly (alkylene *trans*-1,4–cyclohexanedicarboxylate)s with n_{CH_2} = 3, 4, 5, 6 depending on the diol (aliphatic ring)
PEF, PPF, PBF, PPeF, PHF, POF, PNF, PDeF, PDoF = poly (alkylene furanoate)s with n_{CH_2} = 2, 3, 4, 5, 6, 8, 9, 10, 12 depending on the diol (aromatic ring)
PESu, PBSu, PHSu, POSu, PDeSu = poly (1,5-pentylene dicarboxylate)s with n_{CH_2} = 2, 4, 6, 8, 10 depending on the diacid (no ring)
[a] Heating rate 2 K min^{-1} amplitude ± 5 K period 60 s
[b] Heating rate 2 K min^{-1} amplitude ± 5 K period 200 s.

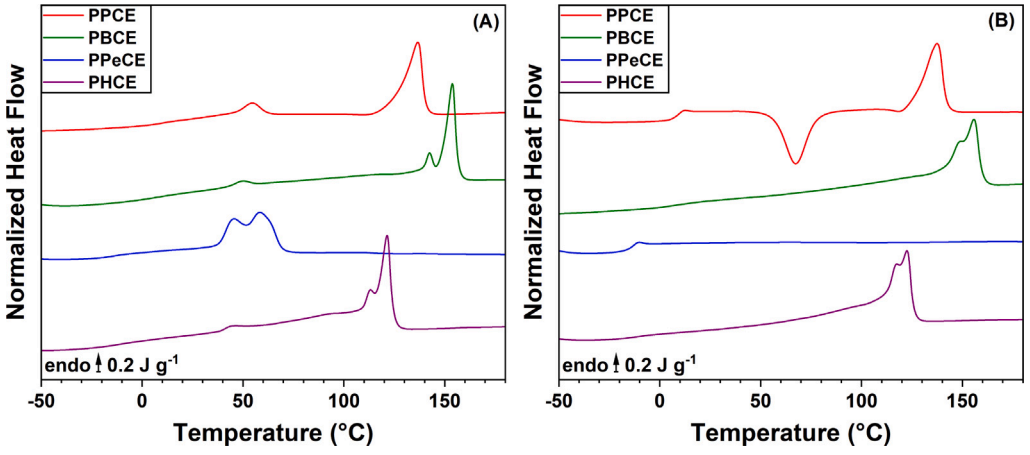

Fig. 3. Preliminary DSC measurements recorded upon heating at 20 K min^{-1} during (A) the 1st scans, and (B) the 2nd scan after cooling at 100 K min^{-1}.

3.2.2. *Glass transition, crystallization ability, melting*

Preliminary DSC measurements were done to evaluate the general thermal behavior of the samples (Fig. 3 (A) 1st scan and (b) 2nd scan). The observed thermal events are listed in Table 3. In the 1st scan, PPCE shows an endothermic deviation of the baseline around 10 °C due to the glass-to-rubber transition of the amorphous phase, followed by two endothermic peaks at higher temperature (40–65 °C and 100–150 °C) attributed to the melting of some crystalline phases. After fast cooling, the glass transition can be detected at 8 °C; the subsequent exothermic inflection at 68 °C corresponds to cold crystallization, followed by a well-defined endothermic peak at 137 °C corresponding to crystal melting. Since $\Delta H_{CC} \approx \Delta H_m$, PPCE could be considered in a fully amorphous state after cooling from the melt at 100 K min^{-1}. The DSC curves recorded for PBCE and PHCE during the 1st and 2nd scans are quite similar, in that they are both characterized by the presence of a double endothermic peak corresponding to the melting of the crystalline phase. The glass transition is barely visible both in the 1st and in the 2nd scans, suggesting a stronger aptitude to crystallize and a more rapid crystal

Table 3
Thermal parameters obtained from the preliminary DSC scans (Fig. 3). T_g is the glass transition temperature (mid-point of the heat capacity step), Δc_p is the specific heat capacity step measured at the glass transition temperature, T_m is the melting temperature (maximum of the melting peak), ΔH_m is the enthalpy of melting, T_{CC} is the cold crystallization temperature (minimum of the crystallization peak), ΔH_{CC} is the enthalpy associated with cold crystallization. For complex melting behaviors, T_m is taken at the maximum of the last peak in the melting temperature range.

	DSC 1st SCAN		DSC 2nd SCAN						
SAMPLE	Glass transition (°C)	Melting (°C)	T_m (°C)	T_g (°C)	Δc_p (J g^{-1} K^{-1})	T_{CC} (°C)	ΔH_{CC} (J g^{-1})	T_m (°C)	ΔH_m (J g^{-1})
PPCE	0–15	40–65, 100–150	137	8	0.294	68	27	137	28
PBCE	−15–15	35–60, 115–165	154	7	0.209	n.o.	n.o.	156	36
PPeCE	−25–0	25–75	57	−13	0.236	n.o.	n.o.	n.o.	n.o.
PHCE	−35–0	35–135	118	−12	0.158	n.o.	n.o.	122	40

PPCE = poly (propylene *trans*-1,4–cyclohexanedicarboxylate)
PBCE = poly (butylene *trans*-1,4–cyclohexanedicarboxylate)
PPeCE = poly (pentamethylene *trans*-1,4–cyclohexanedicarboxylate)
PHCE = poly (hexamethylene *trans*-1,4–cyclohexanedicarboxylate)
n.o. = not observed.

growth in PBCE and PHCE compared to PPCE. The 1st scan of PPeCE shows a glass-to-rubber transition at negative temperatures, followed by a double endothermic peak slightly above room temperature (25–75 °C), suggesting that chain folding is disrupted despite the easiness of molecular motions, and that the grown crystals are thin and defective. The observation of a multiple melting peak could be due to either some melting-crystallization-melting processes occurring during the heating scan (different degrees of crystal perfection) and/or to the presence of more or less ordered phases (different scales of molecular organization). Further analyses are necessary to clarify the origin of the observed phenomena. After fast cooling, only an endothermic step corresponding to glass transition is observed, proving that PPeCE is the easiest to quench out of all the investigated polyesters. Besides PPeCE, all the other samples also exhibit a tiny endotherm signal in the temperature range 35–60 °C of the 1st scan. This peak measured right above room temperature could indicate the presence of a sort of mesophase, possibly arising from a 1D/2D-arrangement due to selective stacking of *cis*- and *trans*- cyclohexane rings according to their preferential boat or chair conformations [43]. In terms of n_{CH_2}, the polyesters containing an even number of methylene groups in the glycolic subunit (PBCE with n_{CH_2} = 4 and PHCE with n_{CH_2} = 6) develop more abundant and thicker crystals, with higher melting temperatures, compared to the polyesters with an odd number of methylene groups (PPCE with n_{CH_2} = 3 and PPeCE with n_{CH_2} = 5). In other words, the overall crystallization ability as well as the crystallization kinetics of these alicyclic polyesters evidence an obvious odd-even effect; a cooling rate of 100 K min^{-1} allowed to quench both PPCE and PPeCE to a fully amorphous state, whereas PBCE and PHCE were able to arrange into some crystalline structures during cooling from the melt, despite the relatively fast cooling conditions. In terms of molecular mobility in the amorphous phase, a decreasing trend in the values of glass transition temperature T_g was expected with an increase in the number of methylene groups n_{CH_2} in the polymer backbone, assuming that chain flexibility increases as the length of its linear aliphatic segments increases and the relative number of stiffer ester groups -C(=O)O- and alicyclic moieties decreases. This prediction would have been totally confirmed if all the samples were quenched to their fully amorphous state, indeed T_g(PPeCE) < T_g(PPCE); instead, the development of a semicrystalline microstructure in PBCE and PHCE produces a confinement effect on the residual amorphous phase, increasing the value of T_g to the one observed for the amorphous (n_{CH_2}-1) samples, with T_g(PBCE) ≈ T_g(PPCE) and T_g(PHCE) ≈ T_g(PPeCE) (Table 3, 2nd scan).

MT-DSC measurements were performed in the attempt of better understanding the thermal events recorded by DSC during the 2nd scan (Fig. 3 (B)). Fig. 4 shows the MT-DSC signals obtained on the samples after melt quenching in liquid nitrogen. Two main behaviors are observed, respectively for the samples containing an odd number of methylene groups (n_{CH_2} = 3 for PPCE and 5 for PPeCE) and the samples containing an even number of methylene groups (n_{CH_2} = 4 for PBCE and 6 for PHCE). In the case of PPCE (Fig. 4(a)) and PPeCE (Fig. 4(c)), a well-defined heat capacity step is observed in the glass transition temperature range, followed by a more or less pronounced cold-crystallization peak and the corresponding melting peak, eventually accompanied by a more or less extensive crystalline reorganization (exothermic events preceding melting). For these samples, the enthalpies associated with cold crystallization and melting are equivalent, supporting the fact that prior to measurement the samples were completely amorphous. Crystalline reorganization and/or melting-crystallization-melting processes are particularly visible and complex in the case of PPCE (Fig. 4(a)), as highlighted by the Non-Reversing Heat Capacity signal as the temperature exceeds 70 °C. Regarding PBCE (Fig. 4(b)) and PHCE (Fig. 4(d)), the heat capacity step at the glass transition is barely visible, which is related to the difficulty encountered in quenching the samples from the molten state, even if liquid nitrogen is used. This is also confirmed by comparing the enthalpies associated with cold crystallization (which is difficult to observe, as it spreads over a large temperature range) and melting. Thus, the ballistic cooling rates applied by quenching samples from the melt into liquid nitrogen allows to obtain amorphous PPCE and PPeCE, but is not sufficient to obtain amorphous PBCE and PHCE. Higher cooling rates are necessary to avoid self-nucleation and crystallization upon cooling from the melt.

FSC experiments were therefore performed with higher values of cooling rate (from 10 to 3 000 K s^{-1}) on much smaller and thinner samples, in the attempt of quenching all the synthesized polyesters from the melt to a fully amorphous glassy state. Finding the exact conditions to obtain a fully amorphous, partially mesomorphic, or partially crystalline polymer may require extended investigations, as already done by Mileva et al. [44] in the case of poly(propylene-*ran*-1-butene) subjected to rapid cooling (hundreds K^{-1}). Increasing the cooling rate could also allow to evidence the formation of mesophase aggregates prior to crystal growth [45]. These aspects, and more specifically the critical cooling rate required to quench these polyesters to a fully amorphous state, are currently explored and partially discussed elsewhere [46]. Here it is worth pointing out that Fig. 4 reveals a strong tendency to undergo crystalline reorganization and/or melting-crystallization-melting processes upon heating, especially in the case of PBCE and PHCE; in the presence of such phenomena, which are kinetically driven, FSC experiments performed with different heating rates (from 1000 to 6000 K s^{-1}) allow to properly characterize the actual semi-crystalline microstructure of the samples prior to the heating scan by suppressing any parasite phenomenon observed at more conventional heating rates [47–50].

Fig. 5 reports the FSC curves recorded upon heating at β^+ = 1000 K s^{-1} (that is to say, 30 000 times faster than the curves recorded by MT-DSC) after cooling at different rates from the molten state. As expected from the comments previously made about Fig. 4, the slowest cooling rate used for FSC experiments (β^- = 10 K s^{-1}) was

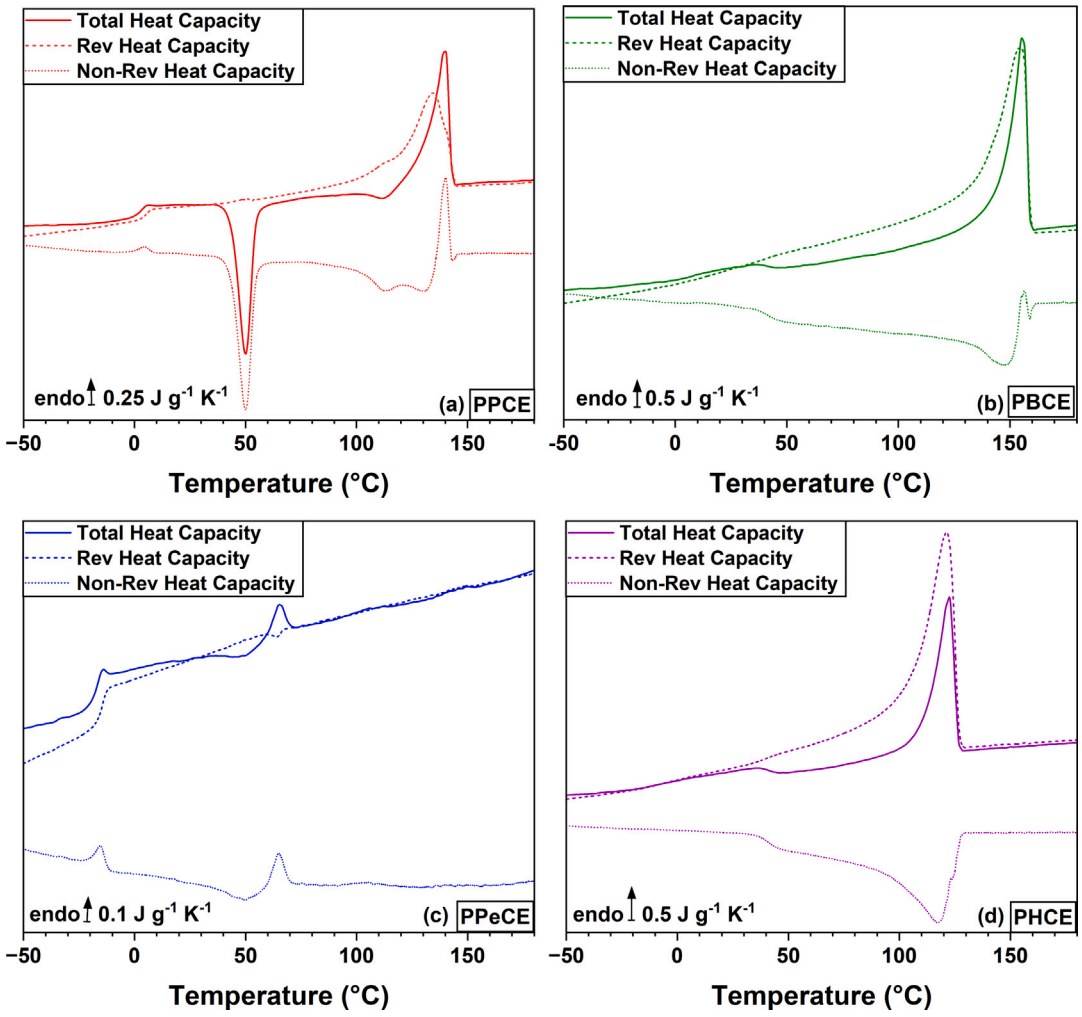

Fig. 4. MT-DSC curves recorded upon heating (1st scan after melt quenching in liquid nitrogen) at 2 K min^{-1} with a modulation amplitude of ± 0.32 K and an oscillation period of 60 s. Blue lines represent the Total Heat Capacity signals, green lines represent the Reversing Heat Capacity signals (i.e. the real component of the complex Heat Capacity response), and red lines represent the Non-Reversing Heat Capacity signal (i.e. the imaginary component of the complex Heat Capacity response). (a) PPCE = poly (propylene *trans*-1,4–cyclohexanedicarboxylate). (b) PBCE = poly (butylene *trans*-1,4–cyclohexanedicarboxylate). (c) PPeCE = poly (pentamethylene *trans*-1,4–cyclohexanedicarboxylate). (d) PHCE = poly (hexamethylene *trans*-1,4–cyclohexanedicarboxylate).

sufficient to obtain fully amorphous samples of PPCE and PPeCE, since the FSC curves subsequently recorded with a heating rate β^+ = 1000 K s^{-1} (Fig. 5(a) for PPCE and Fig. 5(c) for PPeCE) report only the glass transition and no melting. It is interesting to point out that cold crystallization is also completely suppressed when a heating rate β^+ = 1000 K s^{-1} is used for the measurement. On the other hand, PHCE could be successfully and completely quenched from the melt only when a cooling rate β^- = 1000 K s^{-1} was used, as shown by the absence of cold crystallization and/or melting in the measurement subsequently done with a heating rate β^+ = 1000 K s^{-1} (Fig. 5(d)). Regarding PBCE, cold crystallization and melting are observed even with the highest cooling rate used for FSC experiments (β^- = 1000 K s^{-1}, Fig. 5(b)); before the measurement, the sample was not completely amorphous, and a heating rate β^+ = 1000 K s^{-1} is still not enough to avoid cold crystallization, the subsequent crystalline reorganization, and melting. Therefore, a larger range of heating rates was explored specifically for this sample. The best results in terms of quenching without further crystallization upon heating were obtained using a cooling rate β^- = 1000 K s^{-1} and a subsequent heating rate β^+ = 3000 K s^{-1}, as shown in Fig. 6. The differences in the behaviors observed with the same heating rate (β^+ = 1000 K s^{-1}) after quenching with three different cooling rates (β^- = 10, 100 and 1000 K s^{-1}) perfectly illustrates how important is to control the cooling rate of a polymer, especially in the case of PBCE (Fig. 5(b)). Indeed, different glassy states are formed at different cooling rates and supercooling degrees, that may have quite different molecular mobilities with inevitable consequences on the microstructure (aptitude to crystallize, maximum crystallinity and crystallization kinetics) as well as on the structural relaxation and physical ageing [51]. The thermal parameters obtained by MT-DSC and FSC are all summarized in Table 4.

3.2.3. *Enthalpy of melting and structure of the crystalline phase*

Most thermodynamic parameters for newly synthesized polymers are not available in the literature. Cebe et al. [24] and Fosse et al. [25] recently used FSC to estimate the enthalpy of melting of different polymers extrapolated to the ideal case of 100% crystalline samples. The main advantage is that the FSC protocol requires nanoscale samples, so there is no need to synthesize large amounts of each polymer. In particular, the protocol proposed by Fosse et al. [25] applies to any crystallizable polymer for which (i) a two-phase semi-crystalline microstructure with a negligible amount of rigid amorphous fraction can be approached by a suitable annealing treatment, and (ii) a fully amorphous state can be obtained. The enthalpy of melting ΔH_m can then be calculated based on FSC curves recorded after different crystallization times at a given crystallization temperature (previously optimized to reduce the coupling between phases, as shown by Fig. 7),

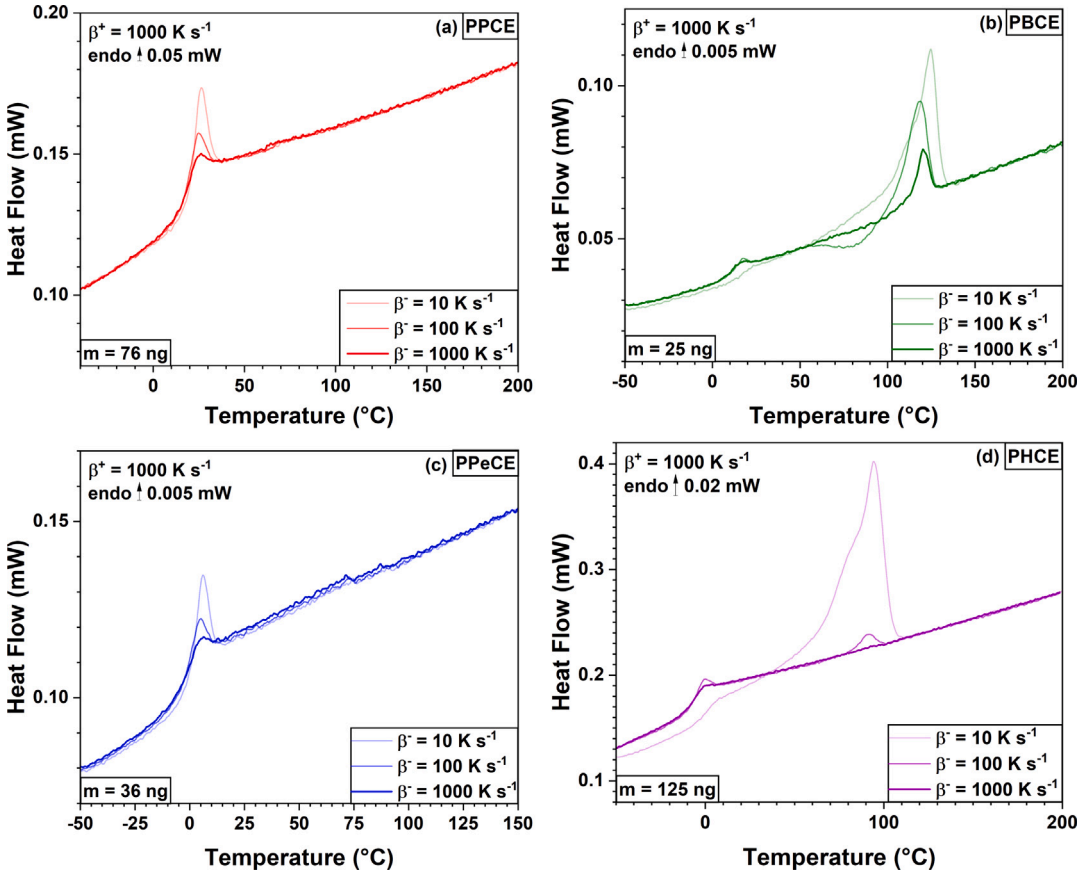

Fig. 5. FSC curves recorded with a heating rate β^+ = 1000 K s^{-1} after quenching from the melt at different cooling rates (β^- = 10 K s^{-1}, 100 K s^{-1} and 1000 K s^{-1}). (a) PPCE = poly (propylene *trans*-1,4–cyclohexanedicarboxylate). (b) PBCE = poly (butylene *trans*-1,4–cyclohexanedicarboxylate). (c) PPeCE = poly (pentamethylene *trans*-1,4–cyclohexanedicarboxylate). (d) PHCE = poly (hexamethylene *trans*-1,4–cyclohexanedicarboxylate).

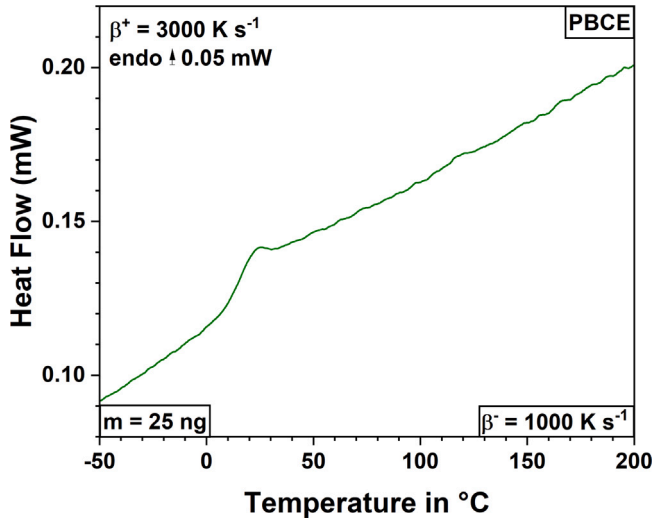

Fig. 6. FSC curve obtained for poly (butylene *trans*-1,4–cyclohexanedicarboxylate) (PBCE) quenched from the melt at a cooling rate β^- = 1000 K s^{-1} and subsequently heated up to 200 °C with a heating rate β^+ = 3000 K s^{-1}.

Table 4
Thermal parameters obtained from both MT-DSC and FSC scans. Δc_p^0 is the heat capacity step measured at the glass transition temperature on a fully amorphous sample [a], T_g is the glass transition temperature (mid-point of the heat capacity step)[b], T_m is the melting temperature (maximum of the melting peak), and ΔH_m^0 is the enthalpy of melting extrapolated to the ideal case of a 100% crystalline sample estimated according to the procedure reported by Fosse et al. [25][c].

SAMPLE	Δc_p^0 (J g^{-1} K^{-1})	T_g^{MT-DSC} (°C)	T_m^{MT-DSC} (°C)	T_g^{FSC} (°C)	T_m^{FSC} (°C)	ΔH_m^0 (J g^{-1})
PPCE	0.27 ± 0.02	5 ± 1	139 ± 1	10 ± 2	140 ± 1	117 ± 10
PBCE	0.19 ± 0.02	n.o.	154 ± 1	5 ± 2	165 ± 1	64/67 ± 10
PPeCE	0.27 ± 0.02	−15 ± 1	65 ± 1	−8 ± 2	73 ± 1	108 ± 10
PHCE	0.16 ± 0.02	n.o.	122 ± 1	−14 ± 2	135 ± 1	61/104 ± 10

[a] The value of Δc_p^0 was measured by MT-DSC (Rev Heat Capacity signal in Fig. 4) after melt quenching. For samples that could not be melt-quenched during MT-DSC measurements, Δc_p^0 was estimated on the basis of FSC measurements.
[b] The T_g values obtained by FSC were corrected for thermal lag according to the recommendations reported in the literature [52].
[c] Two values of ΔH_m^0 are provided for PBCE and PHCE depending on the temperature range used for the calculation (either from $T_{g,end\,set}$ to the melt, or from $T_{m,onset}$ to the melt).
PPCE = poly (propylene *trans*-1,4–cyclohexanedicarboxylate)
PBCE = poly (butylene *trans*-1,4–cyclohexanedicarboxylate)
PPeCE = poly (pentamethylene *trans*-1,4–cyclohexanedicarboxylate)
PHCE = poly (hexamethylene *trans*-1,4–cyclohexanedicarboxylate)
n.o. = not observed.

and the ΔH_m^0 can be approached by extrapolating the experimental data to an ideal 100% crystalline state, which would correspond to $\Delta c_p \approx$ nil (Fig. 8). The values of ΔH_m^0 estimated for PPCE, PBCE, PPeCE and PHCE are reported in Table 4. In a previous work, Gigli et al. [53] could estimate values of T_m^0 = 184 °C and ΔH_m^0 = 78 J g^{-1} for PBCE by applying Baur's equation to a series of poly (butylene *trans*-cyclohexanedicarboxylate-*ran*-diglycolate) copolymers with various compositions. This work provides a preliminary estimation of the values of ΔH_m^0. Further investigations will be needed to improve

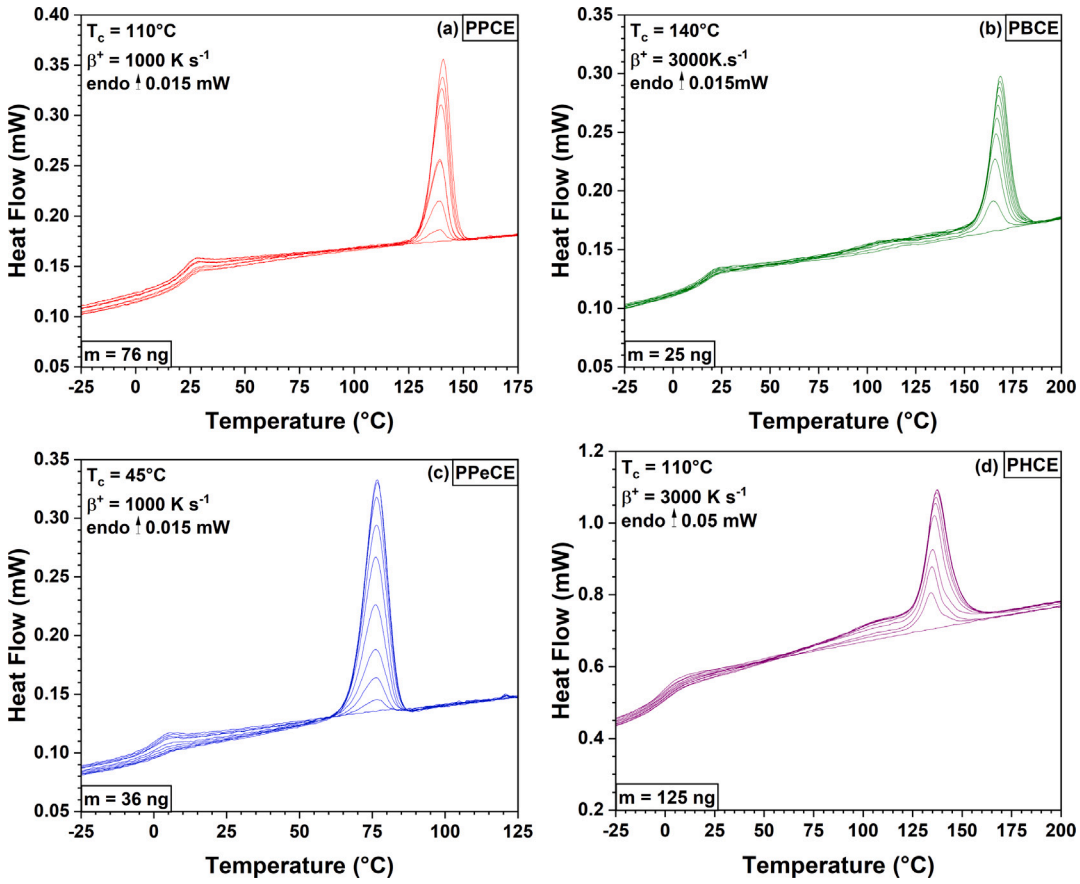

Fig. 7. FSC curves recorded with a heating rate of either 1000 K s^{-1} ((a) and (c)) or 3000 K s^{-1} ((b) and (d)) after melt quenching followed by isothermal crystallization at an appropriate T_C (110 °C for PPCE, 140 °C for PBCE, 45 °C for PPeCE and 110 °C for PHCE) for different times. (a) PPCE = poly (propylene *trans*-1,4–cyclohexanedicarboxylate). (b) PBCE = poly (butylene *trans*-1,4–cyclohexanedicarboxylate). (c) PPeCE = poly (pentamethylene *trans*-1,4–cyclohexanedicarboxylate). (d) PHCE = poly (hexamethylene *trans*-1,4–cyclohexanedicarboxylate).

the accuracy of these results, especially in the case of PBCE and PHCE (Fig. 8(b) and (d)), which seem to be particularly prone to the development of complex microstructures containing mesophases and/or defective crystalline domains, as suggested by the endothermic deviation of the baseline recorded by FSC between the glass transition and the melting temperature ranges (Fig. 7(b) and (d)).

X-ray measurements were performed to compare the crystalline phases of the investigated polyesters and distinguish the samples developing more or less regular/defective crystalline structures. The diffraction profiles recorded for PPCE, PBCE, PPeCE and PHCE are reported in Fig. 9. The values of crystallinity X_C estimated from X-ray measurements are summarized in Table 5, along with the mean size of the crystalline domains l_C calculated with Scherrer's equation and the crystalline inter-planar distance (or average inter-chain distance in the amorphous phase) calculated with Bragg's law.

All the recorded X-ray spectra are quite complex, but some differences are clear. PPCE (Fig. 9(a), n_{CH_2} = 3) and PPeCE (Fig. 9(b), n_{CH_2} = 5) have broader crystalline peaks compared to PBCE (Fig. 9(c), n_{CH_2} = 4) and PHCE (Fig. 9(d), n_{CH_2} = 6), suggesting that the crystalline domains formed in samples with an odd number of methylene groups are smaller and more defective compared to the ones formed in samples with an even number of methylene groups. In particular it appears that, within the investigated series of polyesters, the most defective crystalline structure is formed by PPeCE (Fig. 9(c)) whereas the most extended crystalline structure is observed for PHCE (Fig. 9(d)), which has the sharpest diffraction peaks. It is however difficult to make comparisons without further pushing the structural characterizations, because the diffraction peaks are not shared by all the samples, and therefore different crystalline forms could be expected. Along with DSC measurements, X-ray measurements show that not only the aptitude to crystallize is strongly dependent on n_{CH_2} (Fig. 3 showed that the samples containing an even number of methylene groups have a better crystallizability compared to the samples containing an odd number of methylene units), but also the crystalline perfection and probably the crystallographic arrangement depend on the length of the linear aliphatic segments in the polymer chains. The angular positions of the main diffraction peaks in the range $2\theta \approx$ 10-30° are listed in Table 5 for all the considered samples. In most cases, the diffraction peaks are affected by small angular shifts; sometimes, additional reflection plans are detected. PPeCE (Fig. 9(c)) has the small number of reflection plans, contrarily to PBCE (Fig. 9(b)) that has the largest number of diffraction peaks, including in the angular range around and above 30°; PHCE exhibit a clear diffraction peak at 2θ = 36.6°. It is evident that additional investigations are required to fully elucidate the crystalline structure of these materials. A work has been recently published about the crystal structure of PBCE fibers, evidencing that two different crystal forms are observed depending on the cooling conditions [54]. The more stable α-form, which is observed after slow cooling from the melt (β^- = 4 K min^{-1}), has a triclinic unit cell with parameters a = 5.46 Å, b = 6.89 Å, c = 13.51 Å, α = 138.37°, β = 109.42°, and γ = 63.30°. The β-form is observed after fast cooling and is a metastable phase. In a previous work, Fortunati et al. [55] produced PBCE films by solvent casting and did not observe additional peaks compared to PHCE, suggesting that the growth of isomorphous crystal phases in even-numbered samples is possible but greatly depends on sample preparation and processing conditions.

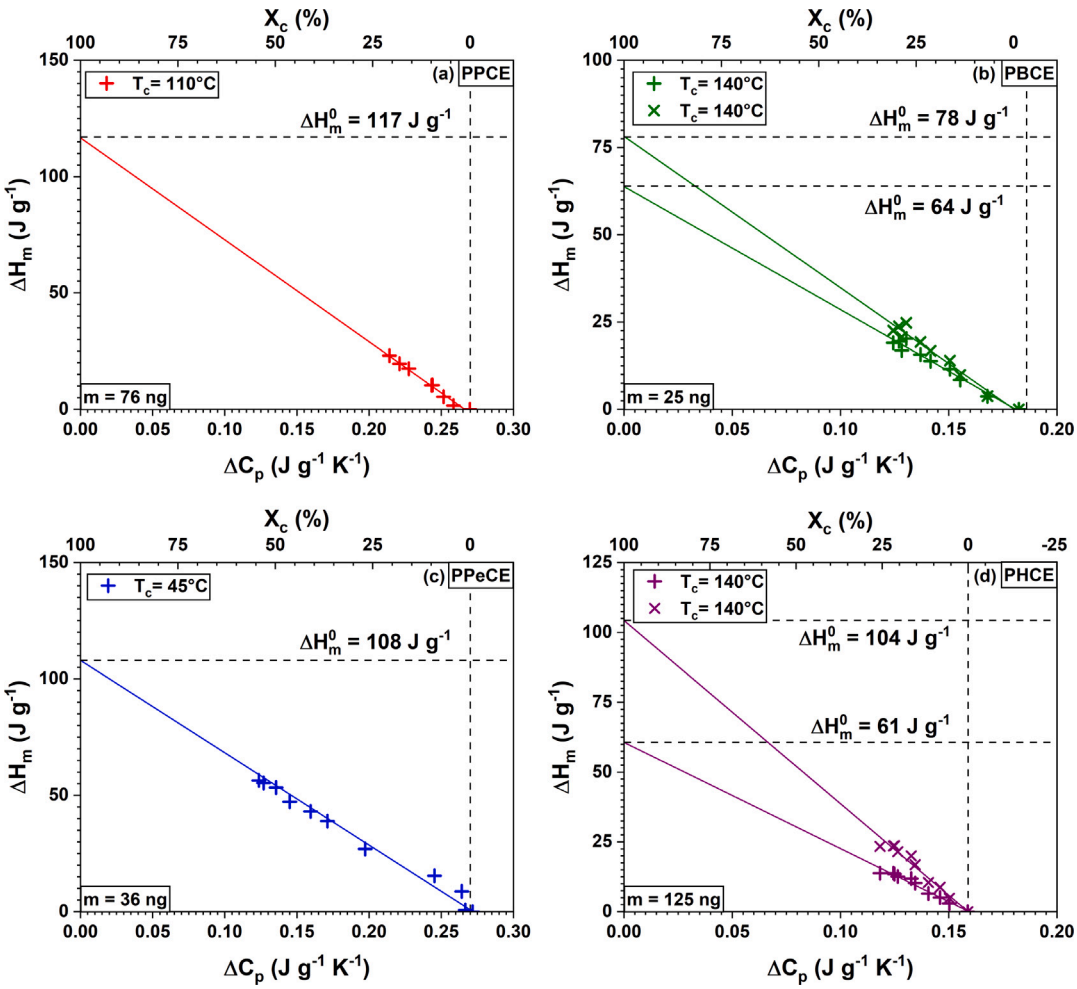

Fig. 8. Estimation of the enthalpy of melting ΔH_m^0 corresponding to the hypothetical 100% crystalline state by extrapolation of the experimental data (ΔH_m vs. ΔC_p) obtained from the FSC curves in Fig. 7 according to the protocol by Fosse et al. [25]. Two values of ΔH_m^0 are provided for PBCE and PHCE depending on the temperature range used for the calculation (either from $T_{g,end\,set}$ to the melt, or from $T_{m,onset}$ to the melt). (a) PPCE = poly (propylene *trans*-1,4–cyclohexanedicarboxylate). (b) PBCE = poly (butylene *trans*-1,4–cyclohexanedicarboxylate). (c) PPeCE = poly (pentamethylene *trans*-1,4–cyclohexanedicarboxylate). (d) PHCE = poly (hexamethylene *trans*-1,4–cyclohexanedicarboxylate).

3.3. Mechanical properties

One representative stress–strain curve for each poly(alkylene *trans*-1,4-cyclo hexanedicarboxylate) sample investigated in this study has been reported in Fig. 10. The corresponding data (Young's modulus E, stress at break σ_{break} and elongation at break ϵ_{break}) are listed in Table 6.

The number of methylene groups in the linear aliphatic segment of the polymer backbone appears to have a significant effect on the mechanical properties. PPCE and PBCE have the highest elastic modulus of all the investigated polyesters, followed by PHCE and PPeCE. Unsurprisingly, the polyester with the poorer crystallization ability (PPeCE) also has the lowest value of Young's modulus. Less obviously, the polyester with the stronger crystallization ability and the less defective crystalline phase (PHCE) does not have the highest value of Young's modulus. It is worth reminding that direct comparisons may be misleading, unless all possible parameters affecting mechanical performances are taken into account. The measurements were performed at room temperature, which means that all the samples were in their rubbery state; this may explain the non-linearity of the stress–strain curves, reducing the estimation of the elastic modulus on a restrained strain range. The overall crystallinity, the crystalline perfection (and therefore the coupling between phases), the molecular mobility (and therefore the difference between room temperature and the glass transition) are all parameters with known influence on the mechanical properties of a polymer [56]. Some of these microstructural features can sometimes counterbalance each other, making it hard to draw conclusions about the exact reasons for similarities or differences in the mechanical behavior. For instance, the lower value of E observed for PHCE compared to PPCE and PBCE could be ascribed to the enhanced chain flexibility (lower T_g) counterbalancing the reinforcing effect due to crystallinity. Similar counterbalancing effects could explain the variation in the T_g values observed for samples in different measurement conditions after different treatments. Apparently, the number of methylene groups n_{CH_2} induces an odd-even effect on the stress at break σ_{break}, whereas it is not really possible to conclude about a direct effect on the elongation at break ϵ_{break} (about 2 to 15 %).

3.4. Barrier properties

Polyesters that are flexible at room or negative temperature could find interesting applications for packaging. For this reason, permeability measurements were performed on the compression-molded films. The values of Gas Transmission Rate (GTR) obtained for all the samples with respect to O_2 and CO_2 are reported in Fig. 11 in comparison with the values reported in the literature for commercial fossil-based packaging materials, as well as biobased and/or biodegradable plastics already available on the market for packaging applications, such as poly (lactic acid) (PLA) and poly (butylene succinate) (PBS). The barrier properties of a polymer depend on several factors. From a microstructural point of view, they are largely affected by (i) the free

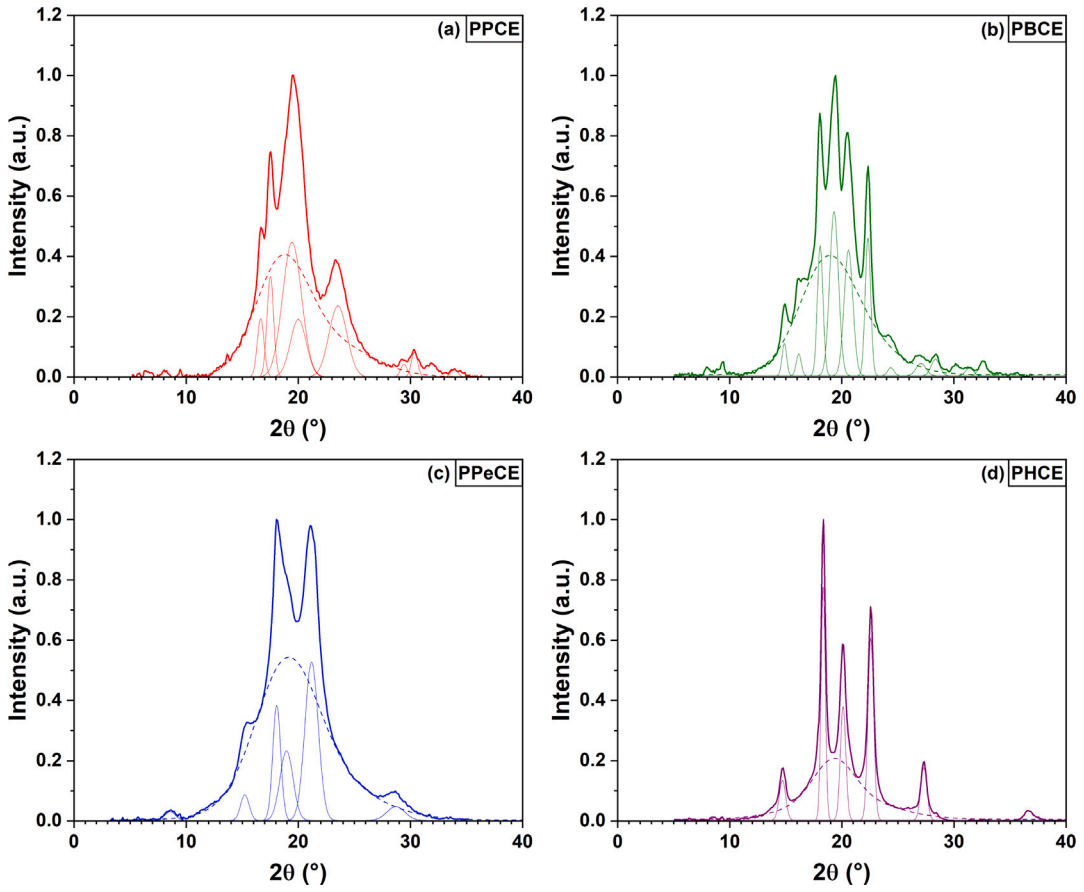

Fig. 9. X-ray spectra recorded on poly(alkylene *trans*-1,4-cyclohexanedicarboxylate)s. The thick solid lines are the experimental curves. The thin solid lines and dotted lines represent the crystalline peaks and the two Gaussian contributions to the amorphous halo. (a) PPCE = poly (propylene *trans*-1,4–cyclohexanedicarboxylate). (b) PBCE = poly (butylene *trans*-1,4–cyclohexanedicarboxylate). (c) PPeCE = poly (pentamethylene *trans*-1,4–cyclohexanedicarboxylate). (d) PHCE = poly (hexamethylene *trans*-1,4–cyclohexanedicarboxylate).

Table 5
Mean size of the crystalline domains l_C and crystalline inter-planar distance (or average amorphous inter-chain distance) d obtained for poly (alkylene *trans*-1,4-cyclohexanedicarboxylate) samples using Scherrer's (Eq. (3)) and Bragg's (Eq. (4)) equations. $FWHM$ is the Full Width at Half Medium of the peaks and 2θ is the angular position of the main crystalline peaks (c1 to c11) and of the two amorphous contributions (am1 and am2).

Peak	c1	c2	c3	c4	c5	c6	c7	c8	c9	c10	c11	am1	am2
PPCE	poly (propylene *trans*-1,4–cyclohexanedicarboxylate)											X_C = 43%	
2θ (°)		16.6	17.5	19.6	20.0		23.5		29.3	30.3		18.5	23.2
$FWHM$ (°)		0.70	0.70	2.1	1.7		1.9		0.70	0.70		4.8	7
l_C (nm)		11	11	4	5		4		12	12			
d (nm)		0.53	0.51	0.45	0.44		0.38		0.30	0.29		0.48	0.38
PBCE	poly (butylene *trans*-1,4–cyclohexanedicarboxylate)											X_C = 36%	
2θ (°)	14.9	16.2	18.1	19.3	20.6	22.3	24.3	27.0	28.0	31.5	32.6	18.6	20.7
$FWHM$ (°)	0.50	0.54	0.60	0.97	0.95	0.56	0.65	1.0	0.9	0.84	0.80	4.8	7
l_C (nm)	16	15	13	8	8	14	12	8	9	10	10		
d (nm)	0.59	0.55	0.49	0.46	0.43	0.40	0.37	0.33	0.32	0.28	0.27	0.48	0.43
PPeCE	poly (pentamethylene *trans*-1,4–cyclohexanedicarboxylate)											X_C = 26%	
2θ (°)	15.2		18.1	19.1	21.1				28.6			18.9	21.2
$FWHM$ (°)	0.95		0.86	1.45	1.46				2.00			5.4	9.5
l_C (nm)	8		9	5	5				4				
d (nm)	0.58		0.49	0.46	0.42				0.31			0.47	0.42
PHCE	poly (hexamethylene *trans*-1,4–cyclohexanedicarboxylate)											X_C = 45%	
2θ (°)	14.6		18.3		20.1	22.6		27.3				19.3	20.5
$FWHM$ (°)	0.67		0.43		0.60	0.65		0.65				4	8
l_C (nm)	12		18		13	12		12					
d (nm)	0.61		0.48		0.44	0.39		0.33				0.46	0.43

volume, whose fraction is larger in the amorphous phase, depends on the temperature and on the easiness of molecular rearrangements, and can therefore be related to T_g, and (ii) the overall amount (ΔH_m, X_C) and quality (T_m, l_C) of the crystalline domains, because the crystalline regions are known to generally be more effective than the amorphous regions in blocking the diffusion of gaseous molecules. According to the

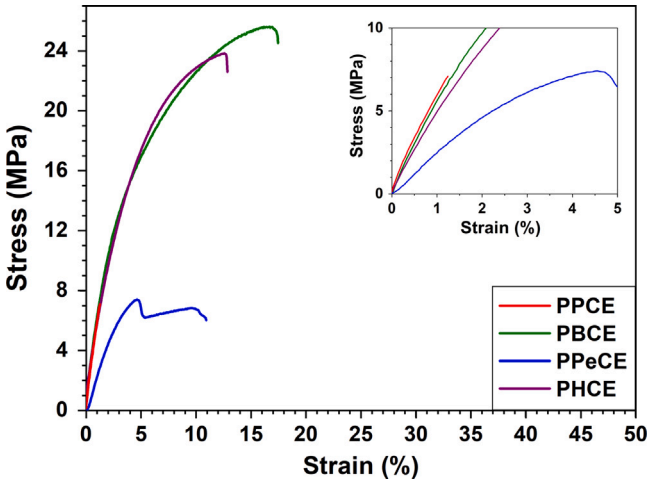

Fig. 10. Stress–strain curves recorded in tensile mode at room temperature with a 10 mm min^{-1} crosshead speed.
PPCE = poly (propylene *trans*-1,4–cyclohexanedicarboxylate). PBCE = poly (butylene *trans*-1,4–cyclohexanedicarboxylate). PPeCE = poly (pentamethylene *trans*-1,4–cyclohexanedicarboxylate). PHCE = poly (hexamethylene *trans*-1,4–cyclohexanedicarboxylate).

Table 6
Mechanical properties obtained from tensile tests performed at room temperature. E is the Young's modulus, σ_{break} is the stress at break, and ϵ_{break} is the elongation at break.

SAMPLE	E (MPa)	σ_{break} (MPa)	ϵ_{break} (%)
PPCE	537 ± 23	8 ± 1	2.0 ± 0.3
PBCE	528 ± 45	23 ± 3	16 ± 4
PPeCE	252 ± 37	7 ± 1	10 ± 3
PHCE	473 ± 47	21 ± 3	12 ± 1

PPCE = poly (propylene *trans*-1,4–cyclohexanedicarboxylate)
PBCE = poly (butylene *trans*-1,4–cyclohexanedicarboxylate)
PPeCE = poly (pentamethylene *trans*-1,4–cyclohexanedicarboxylate)
PHCE = poly (hexamethylene *trans*-1,4–cyclohexanedicarboxylate).

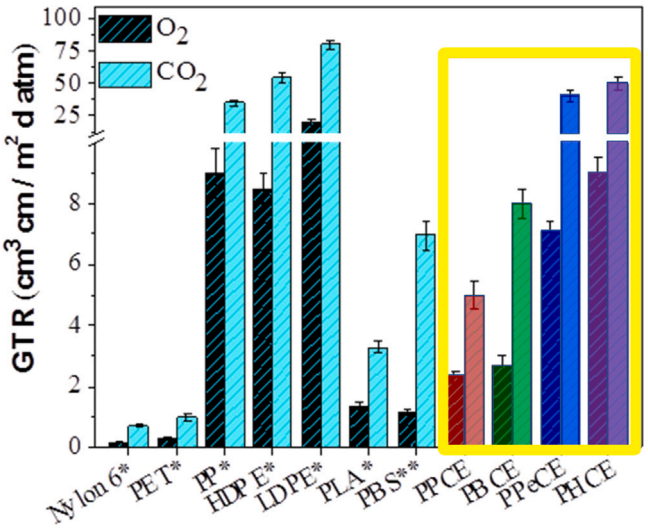

Fig. 11. Gas Transmission Rate (GTR) to O_2 and CO_2 for the investigated poly (alkylene *trans*-1,4-cyclohexanoate)s compared to the values reported in the literature for some traditional petroleum and biobased polymers for packaging. PPCE = poly (propylene *trans*-1,4–cyclohexanedicarboxylate). PBCE = poly (butylene *trans*-1,4–cyclohexanedicarboxylate). PPeCE = poly (pentamethylene *trans*-1,4–cyclohexanedicarboxylate). PHCE = poly (hexamethylene *trans*-1,4–cyclohexanedicarboxylate).
* from Mensitieri et al. [63]
** from Guidotti et al. [64].

results in Fig. 11, PPCE and PBCE are the most performing materials, since their GTR values are the lowest out of the investigated series of polyesters. These two polymers have the highest values of T_g and T_m, respectively, and an overall crystallinity of 43% and 36%. The barrier properties of PPeCE dramatically decrease compared to PPCE and PBCE; the reasons could be a lower value of T_g, and a smaller fraction of more defective crystals. Once again, despite a larger amount of more regular crystals, the barrier properties of PHCE are the worst out of the considered polyesters. This result, which is only apparently surprising, stresses the importance of controlling processing conditions and carefully evaluating all the microstructural features potentially related to free volume and molecular mobility. Guidotti et al. recently reported smart barrier properties for random copolymers containing PBCE-type segments [43] and for camphor-modified PBCE [57]; since cyclohexane is a mesogenic moiety, they supposed the existence of some mesophase (1D/2D-ordered domains) generated by the association of the cyclohexane rings into closely packed structures. In the literature it has been previously reported for propene/ethylene copolymers [58] and poly(butylene 2,5-thiophenate) [59] that the growth of crystalline domains limits the formation of mesophases, which could potentially explain a decrease in the barrier properties in polymers with relatively high crystalline contents. Besides, an increase in the number of methylene groups n_{CH_2} corresponds to a decrease in the relative amount of cyclohexane rings, which further reduces the chances to generate a mesophase. Irrespective of n_{CH_2}, all the investigated polysters exhibit better barrier properties to O_2 compared to CO_2; there is no obvious relationship between permeability and the molecular size of the permeant, since in most polymers CO_2 (molecular diameter 3.4 Å) is more permeating than O_2 (molecular diameter 3.1 Å) [60–62]. The investigated poly (alkylene *trans*-1,4-cyclohexanoate)s have superior barrier properties compared to polyolefins; PPCE and PBCE could even compete with PBS and PLA. It is worth noting that the *cis*-isomer content could also play a role in barrier performance, as evidenced by the results previously published on PBCE with a *cis*-isomer content around 2 mol% [43]. In particular, it was shown that a decrease in the *cis*-isomer content could increase the melting temperature and the overall crystallinity, and these factors both favor the material ability to act as a barrier to gaseous molecules. Besides, a change in the *cis/trans* isomer ratio affects the chances that two or more cyclohexane rings have to stack and generate 1D/2D-ordered domains. Depending on the relative content of the two isomers, the presence of *cis*-isomers is expected to limit the possibility of stacking of *trans*-isomers.

3.5. Compostability

Considering that about 30%–40% of plastic waste comes from packaging, it appeared interesting to evaluate the aptitude of the investigated polyesters to biodegrade in composting conditions. The behavior of PPCE and PBCE had already been reported and discussed in previous studies [65,66], and in both cases no significant weight loss was observed after six months of incubation. The behavior of PPeCE and PHCE seems different, as shown by SEM images (Fig. 12 panel A) and according to the weight loss measured at different incubation times up to three months (Fig. 12 panel B).

The morphological changes at the surface of PPeCE and PHCE films reveal that degradation proceeds through the formation of cracks and holes of increasing size. This process is accompanied by a significant weight loss of the incubated specimens (Fig. 12 panel B). PHCE degrades more slowly compared to PPeCE (the former lost about 4 wt% after 90 days of composting, whereas the latter lost more than 10 wt% after 30 days, reaching 20 wt% after 90 days). The observed trend could be explained by the differences in crystallinity (26% for PPeCE, 45% for PHCE); it is well known that amorphous regions are preferentially degraded with respect to crystalline domains. Moreover, the

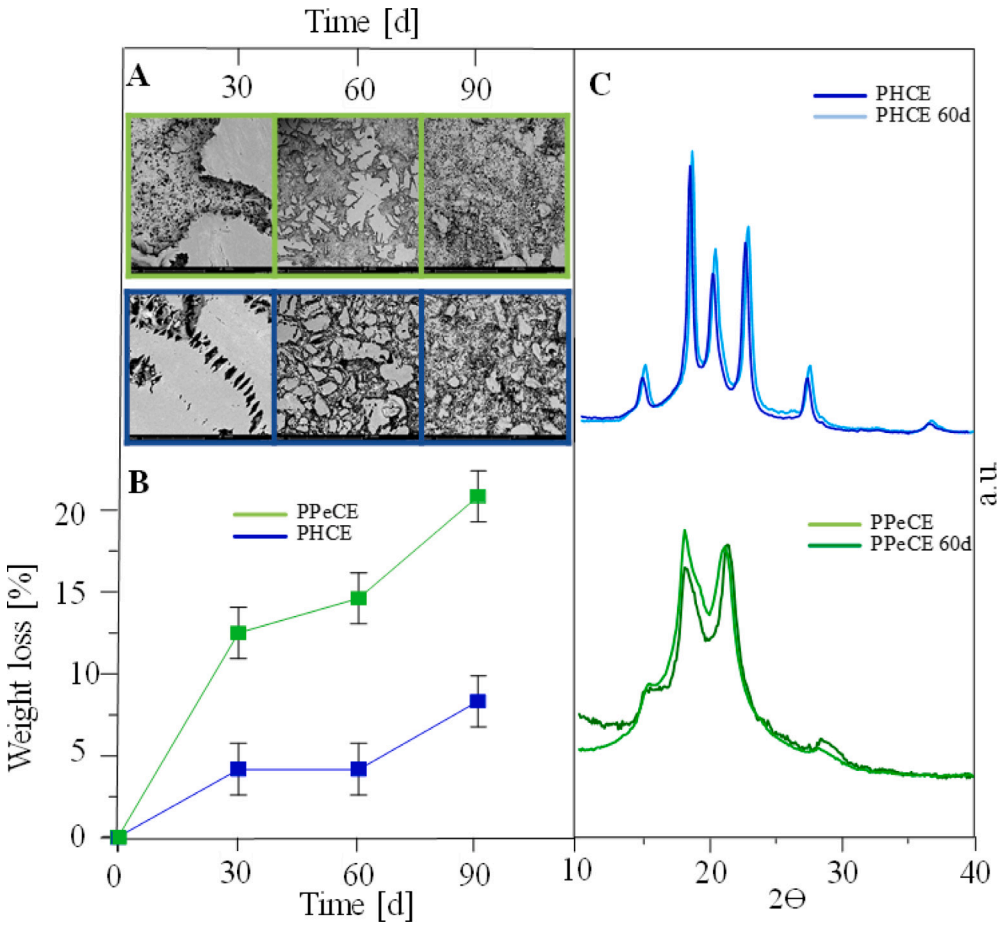

Fig. 12. (A) SEM images of PPeCE and PHCE film surface after 30, 60 and 90 days in composting conditions [2000x]. The initial appearance of film surfaces was flat and smooth (not shown). (B) Weight loss of PPeCE and PBCE as a function of the incubation time. (C) X-ray diffraction patterns recorded on PPeCE and PHCE before the test and after 60 days in composting conditions. PPeCE = poly (pentamethylene *trans*-1,4–cyclohexanedicarboxylate). PHCE = poly (hexamethylene *trans*-1,4–cyclohexanedicarboxylate).

temperature in the composting chamber (58 °C) is in the range where melting of PPeCE crystals occurs, which further favors the degradation process by increasing free volume and molecular mobility. Fig. 12 panel C shows the results of X-rays measurements performed on PPeCE and PHCE films before the test and after 60 days of incubation. The relative intensity and shape of the diffraction peaks slightly change as the composting time increases, suggesting that complex microstructural rearrangements are likely to occur. One may hypothesize either an increase in the overall crystallinity due to the preferential degradation of the amorphous phase (as in the case of PHCE, whose amorphous phase is very mobile and crystalline phase is stable up to 122–135 °C), or a progressive disappearance of the smallest and most defective crystals and the refinement of the more stable ones (as in the case of PPeCE, for which crystalline reorganization and melting is observed at temperatures close to the one experienced during incubation). These results are preliminary and mostly intended to showcase the potentialities of alicyclic polyesters. Further investigations are needed to better evaluate the biodegradability of these materials as a function of sample size and crystallinity, with regards to the composition of their repeating units. It is however interesting to see that the stability of these polyesters in composting conditions, which is known to depend on several parameters including the microstructure, could indirectly be tuned through a control over the chemical composition.

4. Conclusions

A series of poly(alkylene *trans*-1,4-cyclohexanedicarboxylate)s was synthesized with controlled *cis*-monomer contents (<10%), high molecular weights ($\overline{M}_w$ > 71 000 g mol^{-1}), and a variable number of methylene groups in the polymer backbone (n_{CH_2} = 3, 4, 5, 6). The thermal stability of the synthesized polyesters is generally very good and not significantly affected by the number of methylene groups n_{CH_2}. The activation energy for thermal degradation is comparable to the values reported in the literature for aromatic polyesters, and significantly larger than the values reported in the literature for polylactic acid. The glass transition temperature T_g is below room temperature (all the samples are in the rubbery state, i.e. they are all flexible), decreases proportionally to the increase in n_{CH_2}, and changes with crystallinity. An obvious odd-even effect is evidenced on the microstructure, in particular on the aptitude to crystallize. The crystallization of odd-numbered samples is disrupted, whereas the even-numbered samples are prone to a very fast crystallization. The developed microstructure is generally complex, as it depends on both chain flexibility (glass transition) and the intrinsic mesogenic character of the alicyclic moiety. The result is the probable coexistance of different crystalline structures, mesophases, and local molecular arrangements, which is also affected by the *cis/trans* isomerism of the cyclohexane rings. The slowest crystallization and the most defective crystalline phase is observed for poly (pentamethylene *trans*-1,4-cyclohexanedicarboxylate) (n_{CH_2} = 5), whereas the fastest crystallization and the most regular crystalline phase is observed for

poly (hexamethylene *trans*-1,4-cyclohexanedicarboxylate) ($n_{CH_2} = 6$). Preliminary tests provided interesting mechanical and barrier properties, making these polyesters suitable for packaging applications, and a significantly improved compostability for $n_{CH_2} \geq 5$, likely due to the reduced aptitude to crystallize.

CRediT authorship contribution statement

Giulia Guidotti: Writing – review & editing, Validation, Investigation, Formal analysis, Data curation, Writing – original draft. **Clément Fosse:** Visualization, Investigation, Formal analysis, Data curation, Writing – original draft . **Michelina Soccio:** Writing – review & editing, Validation, Supervision, Methodology, Conceptualization, Writing – original draft. **Massimo Gazzano:** Investigation, Formal analysis, Data curation. **Valentina Siracusa:** Investigation, Formal analysis, Data curation. **Laurent Delbreilh:** Validation, Supervision, Resources, Funding acquisition. **Antonella Esposito:** Writing – review & editing, Writing – original draft, Visualization, Validation, Supervision, Project administration, Methodology, Conceptualization. **Nadia Lotti:** Validation, Supervision, Resources, Project administration, Methodology, Funding acquisition, Conceptualization.

Declaration of competing interest

The authors declare that they have no known competing financial interests or personal relationships that could have appeared to influence the work reported in this paper.

Acknowledgments

Thomas Flammang and Brigitte Djuiga Wabo (second-year master students at the University of Rouen Normandie, Sciences de la Matière, Génie des Matériaux) are acknowledged for contributing to polymer synthesis and characterization as interns at the University of Bologna. Silvia Quattrosoldi is acknowledged for contributing to preliminary characterizations.

Data availability

Data will be made available on request.

References

[1] A.R. Ajitha, S. Abitha, Poly(trimethylene terephthalate): Introduction, in: A.R. Ajitha, S. Thomas (Eds.), Poly Trimethylene Terephthalate: Based Blends, IPNs, Composites and Nanocomposites, Springer Nature, Singapore, 2023, pp. 3–9, http://dx.doi.org/10.1007/978-981-19-7303-1_1.

[2] S. Turner, Y. Liu, 5.14 - chemistry and technology of step-growth polyesters, in: K. Matyjaszewski, M. Möller (Eds.), Polymer Science: A Comprehensive Reference, Elsevier, 2012, pp. 311–331, http://dx.doi.org/10.1016/B978-0-444-53349-4.00143-6.

[3] H. Klare, G. Reinisch, The structure and the properties of polyalkylene terephthalates (PATP). a review, Polym. Sci. U.S.S.R. 21 (11) (1979) 2727–2745, http://dx.doi.org/10.1016/0032-3950(79)90378-2.

[4] L. De Vos, B. Van de Voorde, L. Van Daele, P. Dubruel, S. Van Vlierberghe, Poly(alkylene terephthalate)s: From current developments in synthetic strategies towards applications, Eur. Polym. J. 161 (2021) 110840, http://dx.doi.org/10.1016/j.eurpolymj.2021.110840.

[5] S.K. Burgess, O. Karvan, J. Johnson, R.M. Kriegel, W.J. Koros, Oxygen sorption and transport in amorphous poly(ethylene furanoate), Polymer 55 (18) (2014) 4748–4756, http://dx.doi.org/10.1016/j.polymer.2014.07.041.

[6] S.K. Burgess, R.M. Kriegel, W.J. Koros, Carbon dioxide sorption and transport in amorphous poly(ethylene furanoate), Macromolecules 48 (7) (2015) 2184–2193, http://dx.doi.org/10.1021/acs.macromol.5b00333.

[7] S.K. Burgess, G.B. Wenz, R.M. Kriegel, W.J. Koros, Penetrant transport in semicrystalline poly(ethylene furanoate), Polymer 98 (2016) 305–310, http://dx.doi.org/10.1016/j.polymer.2016.06.046.

[8] A. Bourdet, A. Esposito, S. Thiyagarajan, L. Delbreilh, F. Affouard, R.J.I. Knoop, E. Dargent, Molecular mobility in amorphous biobased poly(ethylene 2,5-furandicarboxylate) and poly(ethylene 2,4-furandicarboxylate), Macromolecules 51 (5) (2018) 1937–1945, http://dx.doi.org/10.1021/acs.macromol.8b00108.

[9] A. Bourdet, C. Fosse, M.-R. Garda, S. Thiyagarajan, L. Delbreilh, A. Esposito, E. Dargent, Microstructural consequences of isothermal crystallization in homo- and co-polyesters based on 2,5- and 2,4-furandicarboxylic acid, Polymer 272 (2023) 125835, http://dx.doi.org/10.1016/j.polymer.2023.125835.

[10] V. Tsanaktsis, E. Vouvoudi, G.Z. Papageorgiou, D.G. Papageorgiou, K. Chrissafis, D.N. Bikiaris, Thermal degradation kinetics and decomposition mechanism of polyesters based on 2,5-furandicarboxylic acid and low molecular weight aliphatic diols, J. Anal. Appl. Pyrolysis 112 (2015) 369–378, http://dx.doi.org/10.1016/j.jaap.2014.12.016.

[11] Z. Terzopoulou, V. Tsanaktsis, M. Nerantzaki, G.Z. Papageorgiou, D.N. Bikiaris, Decomposition mechanism of polyesters based on 2,5-furandicarboxylic acid and aliphatic diols with medium and long chain methylene groups, Polym. Degrad. Stab. 132 (2016) 127–136, http://dx.doi.org/10.1016/j.polymdegradstab.2016.03.006.

[12] Z. Terzopoulou, V. Tsanaktsis, M. Nerantzaki, D.S. Achilias, T. Vaimakis, G.Z. Papageorgiou, D.N. Bikiaris, Thermal degradation of biobased polyesters: Kinetics and decomposition mechanism of polyesters from 2,5-furandicarboxylic acid and long-chain aliphatic diols, J. Anal. Appl. Pyrolysis 117 (2016) 162–175, http://dx.doi.org/10.1016/j.jaap.2015.11.016.

[13] G.Z. Papageorgiou, V. Tsanaktsis, D.G. Papageorgiou, K. Chrissafis, S. Exarhopoulos, D.N. Bikiaris, Furan-based polyesters from renewable resources: Crystallization and thermal degradation behavior of poly(hexamethylene 2,5-furandicarboxylate), Eur. Polym. J. 67 (2015) 383–396, http://dx.doi.org/10.1016/j.eurpolymj.2014.08.031.

[14] S. Thiyagarajan, M.A. Meijlink, A. Bourdet, W. Vogelzang, R.J.I. Knoop, A. Esposito, E. Dargent, D.S. van Es, J. van Haveren, Synthesis and thermal properties of bio-based copolyesters from the mixtures of 2,5- and 2,4-furandicarboxylic acid with different diols, ACS Sustain. Chem. Eng. 7 (22) (2019) 18505–18516, http://dx.doi.org/10.1021/acssuschemeng.9b04463.

[15] C. Fosse, A. Esposito, S. Thiyagarajan, M. Soccio, N. Lotti, E. Dargent, L. Delbreilh, Cooperativity and fragility in furan-based polyesters with different glycolic subunits as compared to their terephthalic counterparts, J. Non-Cryst. Solids 597 (2022) 121907, http://dx.doi.org/10.1016/j.jnoncrysol.2022.121907.

[16] L. Silverwood, M. Mottoul, M. Dumont, A review of end-of-life pathways for poly(ethylene furanoate) and its derivatives, J. Polym. Environ. 32 (2024) 4130–4142, http://dx.doi.org/10.1007/s10924-024-03229-1.

[17] F. Wu, M. Misra, A.K. Mohanty, Challenges and new opportunities on barrier performance of biodegradable polymers for sustainable packaging, Prog. Polym. Sci. 117 (2021) 101395, http://dx.doi.org/10.1016/j.progpolymsci.2021.101395.

[18] M. Soccio, N. Lotti, L. Finelli, M. Gazzano, A. Munari, Aliphatic poly(propylene dicarboxylate)s: Effect of chain length on thermal properties and crystallization kinetics, Polymer 48 (11) (2007) 3125–3136, http://dx.doi.org/10.1016/j.polymer.2007.04.007.

[19] C. Zhou, Z. Wei, Y. Yu, S. Shao, X. Leng, Y. Wang, Y. Li, Biobased long-chain aliphatic polyesters of 1,12-dodecanedioic acid with a variety of diols: Odd-even effect and mechanical properties, Mater. Today Commun. 19 (2019) 450–458, http://dx.doi.org/10.1016/j.mtcomm.2019.05.005.

[20] C. Fosse, A. Esposito, P. Lemechko, Y.S. Salim, V. Causin, V. Gaucher, S. Bruzaud, K. Sudesh, L. Delbreilh, E. Dargent, Effect of chemical composition on molecular mobility and phase coupling in poly(3-hydroxybutyrate-co-3-hydroxyvalerate) and poly(3-hydroxybutyrate-co-3-hydroxyhexanoate) with different comonomer contents, J. Polym. Environ. 31 (2023) 4430–4447, http://dx.doi.org/10.1007/s10924-023-02882-2.

[21] G. Guidotti, L. Genovese, M. Soccio, M. Gigli, A. Munari, V. Siracusa, N. Lotti, Block copolyesters containing 2,5-furan and trans-1,4-cyclohexane subunits with outstanding gas barrier properties, Int. J. Mol. Sci. 20 (9) (2019) http://dx.doi.org/10.3390/ijms20092187.

[22] R. Blaine, B. Hahn, Obtaining kinetic parameters by modulated thermogravimetry, J. Therm. Anal. Calorim. 54 (1998) 695—-704, http://dx.doi.org/10.1023/A:1010171315715.

[23] A.A. Lacey, D.M. Price, M. Reading, Theory and practice of modulated temperature differential scanning calorimetry, in: M. Reading, D.J. Hourston (Eds.), Modulated Temperature Differential Scanning Calorimetry: Theoretical and Practical Applications in Polymer Characterisation, Springer Netherlands, Dordrecht, 2006, pp. 1–81, http://dx.doi.org/10.1007/1-4020-3750-3_1.

[24] P. Cebe, D. Thomas, J. Merfeld, B.P. Partlow, D.L. Kaplan, R.G. Alamo, A. Wurm, E. Zhuravlev, C. Schick, Heat of fusion of polymer crystals by fast scanning calorimetry, Polymer 126 (2017) 240–247, http://dx.doi.org/10.1016/j.polymer.2017.08.042.

[25] C. Fosse, A. Bourdet, E. Ernault, A. Esposito, N. Delpouve, L. Delbreilh, S. Thiyagarajan, R.J. Knoop, E. Dargent, Determination of the equilibrium enthalpy of melting of two-phase semi-crystalline polymers by fast scanning calorimetry, Thermochim. Acta 677 (2019) 67–78, http://dx.doi.org/10.1016/j.tca.2019.03.035.

[26] N. Murthy, S. Correale, H. Minor, Structure of the amorphous phase in crystallizable polymers: poly (ethylene terephthalate), Macromolecules 24 (5) (1991) 1185–1189, http://dx.doi.org/10.1021/ma00005a033.

[27] G. Stoclet, R. Seguela, J.M. Lefebvre, S. Elkoun, C. Vanmansart, Strain-induced molecular ordering in polylactide upon uniaxial stretching, Macromolecules 43 (3) (2010) 1488–1498, http://dx.doi.org/10.1021/ma9024366.

[28] P. Scherrer, Nachrichten von der Gesellschaft der Wissenschaften zu Göttingen, Mathematisch-Physikalische Klasse, Göttinger Nachrichten Gesell 2 (1918) 98–100.
[29] W.H. Bragg, W.L. Bragg, The reflection of X-rays by crystals, Proc. R. Soc. Lond. Ser. A Math. Phys. Eng. Sci. 88 (605) (1913) 428–438, http://dx.doi.org/10.1098/rspa.1913.0040.
[30] V. Siracusa, C. Ingrao, Correlation amongst gas barrier behaviour, temperature and thickness in BOPP films for food packaging usage: A lab-scale testing experience, Polym. Test. 59 (2017) 277–289, http://dx.doi.org/10.1016/j.polymertesting.2017.02.011.
[31] V. Siracusa, I. Blanco, S. Romani, U. Tylewicz, P. Rocculi, M.D. Rosa, Poly(lactic acid)-modified films for food packaging application: Physical, mechanical, and barrier behavior, J. Appl. Polym. Sci. 125 (S2) (2012) E390–E401, http://dx.doi.org/10.1002/app.36829.
[32] S. Mrkić, K. Galić, M. Ivanković, S. Hamin, N. Ciković, Gas transport and thermal characterization of mono- and di-polyethylene films used for food packaging, J. Appl. Polym. Sci. 99 (4) (2006) 1590–1599, http://dx.doi.org/10.1002/app.22513.
[33] V. Siracusa, Food packaging permeability behaviour: A report, Int. J. Polym. Sci. 2012 (1) (2012) 302029, http://dx.doi.org/10.1155/2012/302029.
[34] V. Siracusa, L. Genovese, C. Ingrao, A. Munari, N. Lotti, Barrier properties of poly(propylene cyclohexanedicarboxylate) random eco-friendly copolyesters, Polymers 10 (5) (2018) 502, http://dx.doi.org/10.3390/polym10050502.
[35] M. Soccio, M. Costa, N. Lotti, M. Gazzano, V. Siracusa, E. Salatelli, P. Manaresi, A. Munari, Novel fully biobased poly(butylene 2,5-furanoate/diglycolate) copolymers containing ether linkages: Structure-property relationships, Eur. Polym. J. 81 (2016) 397–412, http://dx.doi.org/10.1016/j.eurpolymj.2016.06.022.
[36] J.P. Klein, Z.M. Gdowski, R.A. Register, Controlling thermomechanical behavior of semicrystalline hydrogenated polynorbornene through the *cis-* to *trans-* cyclopentylene ratio, J. Polym. Sci. 60 (2) (2022) 266–275, http://dx.doi.org/10.1002/pol.20210752.
[37] F. Liu, J. Qiu, J. Wang, J. Zhang, H. Na, J. Zhu, Role of cis-1,4-cyclohexanedicarboxylic acid in the regulation of the structure and properties of a poly(butylene adipate-co-butylene 1,4-cyclohexanedicarboxylate) copolymer, RSC Adv. 6 (2016) 65889–65897, http://dx.doi.org/10.1039/C6RA13495E.
[38] J.H. Flynn, L.A. Wall, A quick, direct method for the determination of activation energy from thermogravimetric data, J. Polym. Sci. Part B: Polym. Lett. 4 (5) (1966) 323–328, http://dx.doi.org/10.1002/pol.1966.110040504.
[39] J.H. Flynn, The historical development of applied nonisothermal kinetics, in: R.F. Schwenker, P.D. Garn (Eds.), Thermal Analysis, Academic Press, 1969, pp. 1111–1126, http://dx.doi.org/10.1016/B978-0-12-395734-4.50035-7.
[40] R.D. Bikiaris, N.M. Ainali, E. Christodoulou, N. Nikolaidis, D.A. Lambropoulou, G.Z. Papageorgiou, Thermal stability and decomposition mechanism of poly(alkylene succinate)s, Macromol 2 (1) (2022) 58–77, http://dx.doi.org/10.3390/macromol2010004.
[41] B. Girija, R. Sailaja, G. Madras, Thermal degradation and mechanical properties of PET blends, Polym. Degrad. Stab. 90 (1) (2005) 147–153, http://dx.doi.org/10.1016/j.polymdegradstab.2005.03.003.
[42] O. Wachsen, K. Platkowski, K.-H. Reichert, Thermal degradation of poly-l-lactide—studies on kinetics, modelling and melt stabilisation, Polym. Degrad. Stab. 57 (1) (1997) 87–94, http://dx.doi.org/10.1016/S0141-3910(96)00226-1.
[43] G. Guidotti, M. Soccio, V. Siracusa, M. Gazzano, A. Munari, N. Lotti, Novel random copolymers of poly(butylene 1,4-cyclohexane dicarboxylate) with outstanding barrier properties for green and sustainable packaging: Content and length of aliphatic side chains as efficient tools to tailor the material's final performance, Polymers 10 (8) (2018) http://dx.doi.org/10.3390/polym10080866.
[44] D. Mileva, Q. Zia, R. Androsch, H.-J. Radusch, S. Piccarolo, Mesophase formation in poly(propylene-ran-1-butene) by rapid cooling, Polymer 50 (23) (2009) 5482–5489, http://dx.doi.org/10.1016/j.polymer.2009.09.064.
[45] J.E.K. Schawe, Mobile amorphous, rigid amorphous and crystalline fractions in isotactic polypropylene during fast cooling, J. Therm. Anal. Calorim. 127 (1) (2017) 931–937, http://dx.doi.org/10.1007/s10973-016-5533-4.
[46] K. Hallavant, M. Soccio, G. Guidotti, N. Lotti, A. Esposito, A. Saiter-Fourcin, Critical cooling rate of fast-crystallizing polyesters: The example of poly(alkylene trans-1,4-cyclohexanedicarboxylate), Polymers 16 (19) (2024) http://dx.doi.org/10.3390/polym16192792.
[47] S. Adamovsky, A. Minakov, C. Schick, Scanning microcalorimetry at high cooling rate, Thermochim. Acta 403 (1) (2003) 55–63, http://dx.doi.org/10.1016/S0040-6031(03)00182-5.
[48] A.A. Minakov, D.A. Mordvintsev, C. Schick, Melting and reorganization of poly(ethylene terephthalate) on fast heating (1000 K/s), Polymer 45 (11) (2004) 3755–3763, http://dx.doi.org/10.1016/j.polymer.2004.03.072.
[49] A. Toda, R. Androsch, C. Schick, Insights into polymer crystallization and melting from fast scanning chip calorimetry, Polymer 91 (2016) 239–263, http://dx.doi.org/10.1016/j.polymer.2016.03.038.
[50] A. Esposito, N. Delpouve, V. Causin, A. Dhotel, L. Delbreilh, E. Dargent, From a three-phase model to a continuous description of molecular mobility in semicrystalline poly(hydroxybutyrate-co-hydroxyvalerate), Macromolecules 49 (13) (2016) 4850–4861, http://dx.doi.org/10.1021/acs.macromol.6b00384.
[51] M. Mejres, K. Hallavant, G. Guidotti, M. Soccio, N. Lotti, A. Esposito, A. Saiter-Fourcin, Physical aging of a biodegradable alicyclic polymer: poly (pentamethylene trans-1,4-cyclohexanedicarboxylate), J. Non-Cryst. Solids 629 (2024) 122874, http://dx.doi.org/10.1016/j.jnoncrysol.2024.122874.
[52] J.E. Schawe, S. Pogatscher, Material characterization by fast scanning calorimetry: Practice and applications, in: C. Schick, V. Mathot (Eds.), Fast Scanning Calorimetry, Springer International Publishing, 2016, pp. 3–80, http://dx.doi.org/10.1007/978-3-319-31329-0_1.
[53] M. Gigli, N. Lotti, M. Gazzano, V. Siracusa, L. Finelli, A. Munari, M. Dalla Rosa, Fully aliphatic copolyesters based on poly(butylene 1,4-cyclohexanedicarboxylate) with promising mechanical and barrier properties for food packaging applications, Ind. Eng. Chem. Res. 52 (36) (2013) 12876–12886, http://dx.doi.org/10.1021/ie401781d.
[54] W. Hu, T. Ma, Y. Zhou, M. Soccio, N. Lotti, D. Cavallo, D. Wang, G. Liu, Crystal structure and polymorphism of poly(butylene-trans-1,4-cyclohexane dicarboxylate), Macromolecules 57 (9) (2024) 4374–4384, http://dx.doi.org/10.1021/acs.macromol.4c00234.
[55] E. Fortunati, M. Gigli, F. Luzi, N. Lotti, A. Munari, M. Gazzano, I. Armentano, J. Kenny, Poly(butylene cyclohexanedicarboxylate/diglycolate) random copolymers reinforced with SWCNTs for multifunctional conductive biopolymer composites, eXpress Polym. Lett. 10 (2) (2016) 111–124, http://dx.doi.org/10.3144/expresspolymlett.2016.12.
[56] J. Li, Z. Zhu, T. Li, X. Peng, S. Jiang, L.-S. Turng, Quantification of the Young's modulus for polypropylene: Influence of initial crystallinity and service temperature, J. Appl. Polym. Sci. 137 (16) (2020) 48581, http://dx.doi.org/10.1002/app.48581.
[57] G. Guidotti, G. Burzotta, M. Soccio, M. Gazzano, V. Siracusa, A. Munari, N. Lotti, Chemical modification of poly(butylene trans-1,4-cyclohexanedicarboxylate) by camphor: A new example of bio-based polyesters for sustainable food packaging, Polymers 13 (16) (2021) http://dx.doi.org/10.3390/polym13162707.
[58] D. Cavallo, F. Azzurri, R. Floris, G.C. Alfonso, L. Balzano, G.W. Peters, Continuous cooling curves diagrams of propene/ethylene random copolymers. The role of ethylene counits in mesophase development, Macromolecules 43 (6) (2010) 2890–2896, http://dx.doi.org/10.1021/ma902865e.
[59] G. Guidotti, M. Gigli, M. Soccio, N. Lotti, M. Gazzano, V. Siracusa, A. Munari, Ordered structures of poly(butylene 2,5-thiophenedicarboxylate) and their impact on material functional properties, Eur. Polym. J. 106 (2018) 284–290, http://dx.doi.org/10.1016/j.eurpolymj.2018.07.027.
[60] L. Piergiovanni, S. Limbo, Food packaging - materiali, tecnologie e soluzioni, Springer Milano, 2010, http://dx.doi.org/10.1007/978-88-470-1457-2.
[61] G.L. Robertson, Optical, mechanical and barrier properties of thermoplastic polymers, in: Food Packaging: Principles and Practice, 3rd Edition, Taylor & Francis Group, CRC Press, 2013, pp. 91–130, http://dx.doi.org/10.1201/b21347-9.
[62] S. Matteucci, Y. Yampolskii, B.D. Freeman, I. Pinnau, Transport of gases and vapors in glassy and rubbery polymers, in: Materials Science of Membranes for Gas and Vapor Separation, John Wiley & Sons, 2006, pp. 1–47, http://dx.doi.org/10.1002/047002903X.ch1.
[63] G. Mensitieri, E. Di Maio, G.G. Buonocore, I. Nedi, M. Oliviero, L. Sansone, S. Iannace, Processing and shelf life issues of selected food packaging materials and structures from renewable resources, Trends Food Sci. Technol. 22 (2) (2011) 72–80, http://dx.doi.org/10.1016/j.tifs.2010.10.001, New challenges in food preservation..
[64] G. Guidotti, M. Soccio, V. Siracusa, M. Gazzano, E. Salatelli, A. Munari, N. Lotti, Novel random PBS-based copolymers containing aliphatic side chains for sustainable flexible food packaging, Polymers 9 (12) (2017) http://dx.doi.org/10.3390/polym9120724.
[65] L. Genovese, N. Lotti, M. Gazzano, L. Finelli, A. Munari, New eco-friendly random copolyesters based on poly(propylene cyclohexanedicarboxylate): Structure-properties relationships, eXPRESS Polym. Lett. 9 (2015) 972–983, http://dx.doi.org/10.3144/expresspolymlett.2015.88.
[66] M. Gigli, N. Lotti, M. Gazzano, V. Siracusa, L. Finelli, A. Munari, M.D. Rosa, Biodegradable aliphatic copolyesters containing PEG-like sequences for sustainable food packaging applications, Polym. Degrad. Stab. 105 (2014) 96–106, http://dx.doi.org/10.1016/j.polymdegradstab.2014.04.006.